OPTIMIZING A FLYWHEEL FOR RESIDENTIAL USE IN SACRAMENTO

A Thesis

Presented to the faculty of the Department of Mechanical Engineering

California State University, Sacramento

Submitted in partial satisfaction of
the requirements for the degree of

MASTER OF SCIENCE

in

Mechanical Engineering

by

Maria Loise Lani Lausterer

SPRING
2020

OPTIMIZING A FLYWHEEL FOR RESIDENTIAL USE IN SACRAMENTO

A Thesis

by

Maria Loise Lani Lausterer

Approved by:

_____, Committee Chair
Hong - Yue (Ray) Tang, Ph.D.

_____, Second Reader
Timothy Marbach, Ph.D.

_____
Date

Student: Maria Loise Lani Lausterer

I certify that this student has met the requirements for format contained in the University format manual, and this thesis is suitable for electronic submission to the library and credit is to be awarded for the thesis.

_____, Graduate Coordinator _____
Troy D. Topping, Ph.D. Date

Department of Mechanical Engineering

Abstract

of

OPTIMIZING A FLYWHEEL FOR RESIDENTIAL USE IN SACRAMENTO

by

Maria Loise Lani Lausterer

Renewable energy technology such as solar energy has variable outputs. Examples of variable outputs are situations where there is cloud coverage or there is not a balance between supply and demand. Energy storage, specifically a flywheel, has great potential for smoothing out the power supply from solar panels and trying to balance fluctuating energy. Flywheels have been around for centuries to serve as a means to store energy. A flywheel power plant can power a city, but if the plant were to stop supplying energy, the entire city would be affected. If each house had its own flywheel and one unit were to stop working, the other flywheels would not be affected and would therefore continue running. The primary goal of this research is to design an optimized flywheel and solar panel unit based on the amount of energy production needed. The components optimized are the size and geometry of the flywheel based on energy consumption data of a house in Sacramento, California. According to SMUD, the average yearly energy consumption of a residential home in Sacramento is about 10,000-kilowatt hour. Based on this value, a flywheel made out of either 1026 carbon steel or T1000G/epoxy with the dimensions 36” ID by 48” OD by 48” in height will both be able to reach the energy consumption value so long as there are 129 and 10 units respectively. The flywheel is designed to be coupled

with a solar panel. The flywheel stores excess energy from the solar panel and uses it to provide energy to the home when the solar panel cannot provide a sufficient amount.

_____, Committee Chair
Hong-Yue (Ray) Tang, Ph.D.

_____
Date

ACKNOWLEDGEMENTS

I would like to thank my family and friends for supporting me and believing in me. I could not have done this without all of you. Mom and Dad, thank you for allowing me to further my education and for being my number one supporters. Thank you to Jared for helping through these trying times and keeping me calm. Thank you to Dr. Tang and Dr. Marbach for taking the time to help me. I greatly appreciate all of you!

TABLE OF CONTENTS

LIST OF TABLES

LIST OF FIGURES

CHAPTER 1

Introduction

1.1 Thesis Objective

The objective of this research is to optimize a flywheel energy storage system (FESS) to reach the energy production value of a house in Sacramento. A manufactured FESS will be the first to be tested to see if it is able to reach the energy production value. Then, larger scaled FESS designs as well as ones made of a carbon fiber material will be tested to see if they can reach the energy production value. The manufactured FESS is the only one that will undergo speed tests to observe the response of the system. This research is not only applicable to Sacramento, but to other cities as well. This is possible by changing the energy consumption value to reflect that city.

1.2 History of Flywheels

The oldest invention of FESS's dates back to 6000 BC where mass moment of inertia was first being used in the production of threads. Spindles with a wooden stick as an axis and a stone, wood, metal, clay, glass or bones with a center hole as the mass. The fibers were rotated by the directly suspended spindle and momentum. The next application of flywheels is the potter's wheel which came around in 4000 BC [1]. After this, flywheels were integrated into spinning wheels which were driven by a running board and shaft. In the Middle Ages, the inertia of large flywheels was used in water and windmills to make up for the unstable driving force. This idea of smoothing unsteady forces was greatly used

in the first industrial revolution. Flywheels were used in steam engines and tool drives to keep machines running smoothly from one cycle to the next. The one-cylinder steam, diesel road rollers, and eccentric presses are some examples. Flywheels in the 19th century were used in internal combustion engines for transmitting piston forces on the drive train. In 1883, the first flywheel energy storage used solely for energy storage, was developed by John A. Howell for military applications. It was in the early 20th century when modern developments were beginning to arise [1].

A flywheel energy storage is a mechanical storage device, also known as a "mechanical battery", that stores electrical energy by converting it to mechanical energy. The flywheel stores the electrical energy in the form of rotational kinetic energy. Typically, the electrical energy comes from the grid, but it could also be any other source of electrical energy such as from a solar panel. The flywheels speeds up as it stores energy from the electric source, and slows down when it is supplying energy to another source [2]. Hence, the flywheel charges when there is excess power, and discharges when power is needed elsewhere.

1.3 Flywheel Energy Storage and Renewable Energy Systems

Renewable energy technologies are continuously growing and expanding, and it is at its highest ever. Renewable energy is one-third of the global power capacity according to the International Renewable Energy Agency (IRENA). This trend over the last five years shows great promise of renewable power being the driver of global energy transformation [3]. In order to keep up with this trend, there must be a way to balance electrical supply

and demand. Despite the advantages of renewable energy, its dependence on its working environment and its intermittent power supply provides challenges for the reliability of renewable energy systems. A storage device such as a FESS can convert and store electrical energy and convert it back to electrical energy when needed. This can be beneficial in terms of compensating for the fluctuating energy production of renewable energy systems [2]. In this case, a FESS will be paired with a photovoltaic system.

FESS can also be beneficial with helping alleviate the effect of the increasing energy prices. Energy demands continue to increase, resulting in increased energy prices especially during what is called peak time. Peak time is when the demand and cost of electricity is at its highest. Peak times vary depending on the utility company [4]. For non-summer months, peak time is from 5 p.m. to 8 p.m. Monday through Friday for residents with Sacramento Municipal Utility District (SMUD) as their electric utility company [5]. An entire breakdown of SMUD's peak times is shown in Figure 1 below [6].

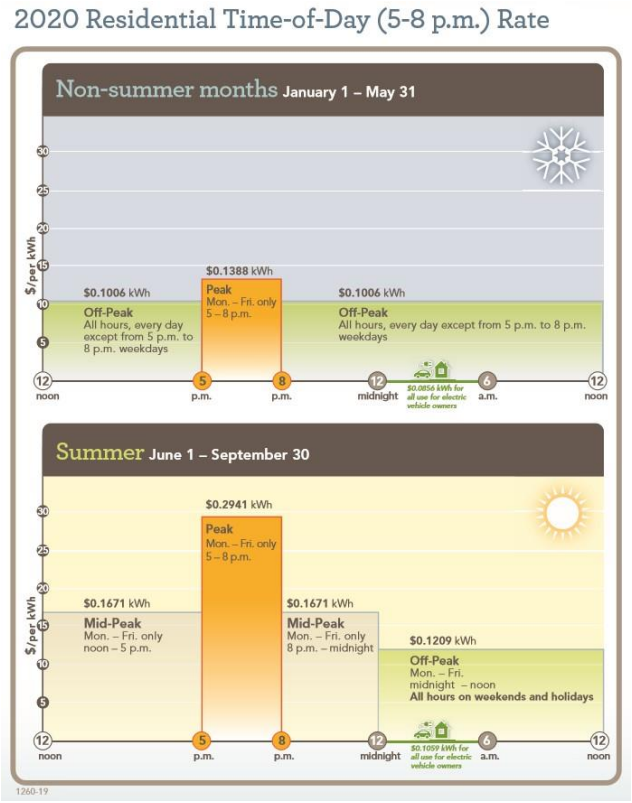

Figure 1. SMUD's peak times

For non-summer months, storing energy during off-peak times where electricity costs about 10 cents per kilowatt-hour (kWh) and storing it until the evening where electricity is worth about 14 cents per kWh saves money for the customer. This is especially true in the summer where electricity during peak time costs more than twice the cost of off-peak time. It is also beneficial because there is a great excess of solar energy during off-peak times when most people are at work or school. According to an economic analysis done by Clean Energy Group, a nonprofit organization working towards a clean energy future, adding storage to California's affordable rental housing almost doubles the electricity bill savings compared to savings from solar alone [7].

The increased number of solar panels being used created a challenge for utilities to balance the supply and demand of the grid. This created what is known as the duck curve due to the curve's resemblance to a duck. The duck curve was first discovered in 2008 when researchers at the National Renewable Energy Laboratory notice a change in their modeling [8]. An image of the duck curve is shown in Figure 2 below. Once the sun sets, energy production needs to be quickly generated since solar panels are not able to provide energy [9]. This is shown in the right portion of Figure 2 and is the head of the duck.

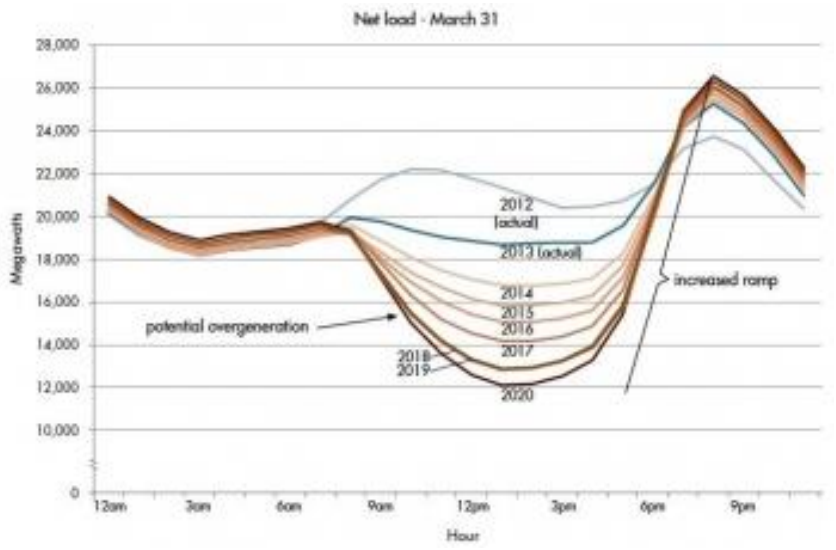

Figure 2. Duck curve

Another challenge caused by the increase in solar panels, is the possibility of solar panels generating more energy than what is being used. This is called over-generation and is shown in the middle portion of the curve in the figure above and is the body of the duck. FESS's can assist in this overgeneration and sudden increase in ramping by storing the extra energy and saving it for when the sun sets, and solar panels can no longer provide energy.

Advances in energy storage show a shift towards energy storage since it is environmentally friendly and cost-effective compared to gas-fired peaker power plants which are plants that only run when there is a high demand. This shift has started appearing at the state level. In September 2017, the state of California enacted SB 338 which directed utilities to evaluate how energy storage could be used as an alternative to gas generation for meeting peak energy demands. Massachusetts quickly followed in California's footsteps and introduced a clean peak standard that required all retail energy suppliers to provide a certain amount of sales from clean peak energy resources. Energy storage systems, including flywheels, are continuing to be favored as a quick, reliable and cost-effective solution to flatten the duck curve [10].

1.4 Solar Panel Instability

The efficiency of solar panels varies throughout the day depending on the weather. Some of the main causes of variabilities are produced by wind speeds and cloud coverage. Cloud cover reduces the amount of sunlight that reaches the solar panels. A cloud crossing the sun can reduce the sunlight by 80% in one second [11]. Solar irradiance is the amount of electromagnetic radiation that penetrates a solar panel per unit area [12]. Wind speed affects how much cloud movements occur which cause rapid fluctuations in solar irradiance. An example of a rapid fluctuation due to cloud movement is shown in Figure 3 [11].

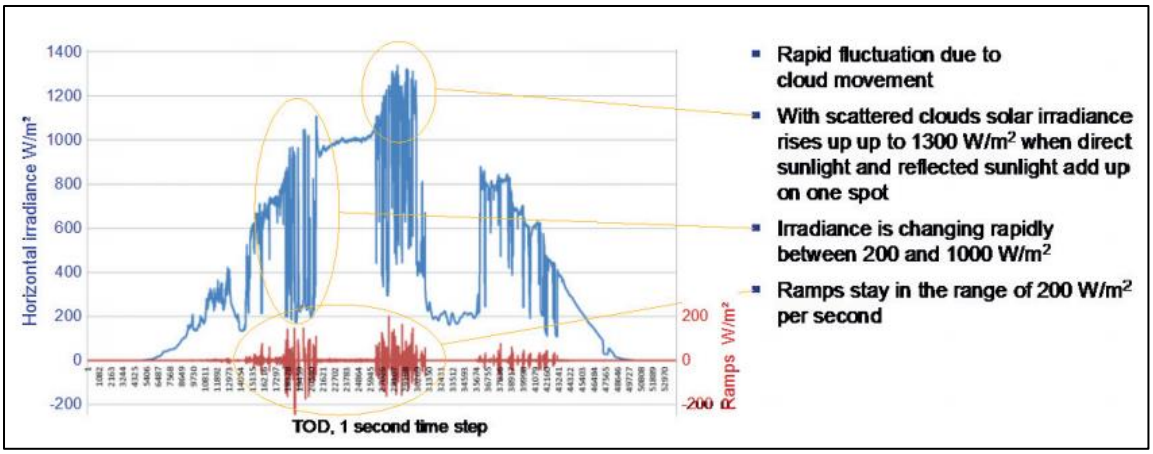

Figure 3. Global horizontal solar irradiance measurement on a cloudy day in Oahu, Hawaii

The measurements of global solar irradiance are in blue while the changes in irradiance, measured in ramps, are in red. There are multiple instances where irradiance changes rapidly between 200 and 1000 $\frac{W}{m^2}$. In this case, the maximum ramp of 200 $\frac{W}{m^2}$ is still a concern for utilities [11]. This rapidly changing solar irradiance presents an issue regarding the power grid because of problems the utilities experience such as efficiency and reliability. Energy Storage Systems were introduced to reduce the effects of rapidly changing solar irradiance on the power grid and to maintain voltage and frequency [13].

Solar efficiency also depends on peak hours, season, and geography. Each affect how much solar irradiance is collected. Peak sun hours refer to how much solar energy is available in an area during a typical day. Peak specifically is when the sun intensity is 1000 watts per square meter [14]. Peak solar radiation occurs when the sun is highest in the sky, called solar noon. At sunrise and sunset, the sun is at a low angle which allows the atmosphere to

filter the sunlight more which means less energy is harnessed. The sun's position is higher in the sky during summer which means there are more hours of sunshine and therefore more solar radiation to harness. As for geography affecting how much solar irradiance is collected, solar energy increases near the equator since it is closer to the sun [14]. Factors such as peaks hours, season, and geography cause solar irradiance generation to be highly variable which causes changes such as that in Figure 3. These variabilities have been of interest for a long time, and they are still being addressed as issues of solar efficiency.

Solar panels do not work at night or during instances such as cloud coverage since they cannot harness energy without the sun. Once the sun sets, all electricity comes from the utility grid. The same goes for when weather interrupts the solar power generation in that the electricity comes from the utility grid. People usually work during the day, so they are not home to use the solar power generated. Some of the solar power generated during this time is wasted because there is no one home to use it. Load shifting puts this wasted solar power to use by storing it in a battery. Load shifting uses excess solar power generated to charge a battery during the day, and later uses this power when it is needed such as at peak times or when weather interrupts energy generation. Load shifting can also be used for periods of increased loading. In increased loading, there would be more energy used than there is energy being generated. In this situation, the battery would supply additional power until there is enough energy being generated by the solar panels to support the energy needed by the house [15]. Load shifting using a battery is the ideal way to maximize energy

during the day, and to solve the problem of inconsistent weather, increased loading, and wasted energy during the day.

Electricity price variation is also an issue for solar energy customers depending if they have what is called a Time-of-Day (TOD) Rate. A TOD Rate is when a customer pays different rates based on the season and or the time of day. Rates increase when the demand and cost for electricity increase. Demand and cost are highest during the summer. Rates are low during off-peak hours since it costs less to produce or purchase electricity [5]. According to the California Public Utilities Commission, all commercial, industrial and agricultural customers in California are required to be on a TOD plan [16]. According to SMUD, the TOD rate became the standard rate for all residential customers in 2019 [5]. Tiered utility rates can also pose issues like the TOD rate. Tiered utility rates are structured so that the more electricity a customer uses, the higher the rate. Once the customer exceeds the electricity amount in a tier, they move to the next tier where the price is higher [17].

Integrating a FESS with one or multiple solar panels allows the storage system to store excess energy collected by the solar panel(s) and counteract the power production drops. While no FESS and solar panel unit currently exists on the market, there are FESS's. Amber Kinetics flywheels work easily with solar panels, not included, and are low-cost and have a 30-year design life [18]. Their M160 flywheel has a target price of $300 to $325 [19].

1.5 Alternative Energy Storage Methods

An advantage for integrating a FESS with a photovoltaic system for household purposes is that it can provide efficient production control and good power management with energy saving and smooth power grids [20]. A big issue that comes with the use of solar panels is their power production curve fluctuates depending on cloud coverage. This fluctuation affects how smooth the power output is. Modern solutions for this issue include the use of chemical batteries to store the excess energy from solar panels. Nowadays, flywheels and batteries are practical energy storage technologies for situations where energy must be stored for use at a later time. An example being Amber Kinetics, an American company that specializes in FESS technology, flywheel which stores energy and discharges it when needed over a 4-hour duration [18]. In comparison to chemical batteries, FESSs have higher energy densities, higher maximum peak power and higher efficiency [20]. Chemical batteries do not have a long service life and contain many materials and acids that are hazardous to humans and the environment [21].

CHAPTER 2

Background

The need to store electric energy is rapidly growing both for improving power quality and accommodating distribution generation. FESS would be beneficial in satellites, space stations, and space vehicles since the sun is their primary source of energy and they are not always in the sun. The energy stored in the FESS would be used for parts of the orbit when the satellites, space stations, and space vehicles are in darkness. In recent military affairs, plans for the U.S. Navy and the U.S. Army to depend more on electricity to propel their ships, manned, unmanned vehicles, weapons navigation, communications, and intelligence systems.

In recent years, FESS has been tested on and modeled to improve certain aspects such as lowering ripple effects or minimizing motor losses. Research suggests there have not been successful attempts at flywheels operating at high speeds since the system overheats. It is possible a cooling system may be needed for a flywheel system to be operational for a larger range of speeds [22]. The purpose of this research is to investigate possible improvements and parametric designs of a FESS and a solar panel unit.

Today, various FESS designs have had safety concerns due to accidents during the past 20 years. The most critical failure modes of FESS's are typically associated with the rotating components such as the rotor, motor and bearings. Typically, the highest possible

rotor speed is wanted in order to produce the highest amount of energy. In order to minimize the initial risk of rotor failure, the maximum allowable speed and stress needs to be determined while setting a safety factor which is typically two. In addition to ageing, material defects such as voids, cracks or segregations can cause premature FESS failure. These defects can be detected and assessed by using non-destructive testing [23]. By detecting these defects, rotor failures can be prevented.

2.1 Flywheel Kinematics

According to Newton's laws, an object in motion tends to stay in motion unless compelled by an external force to act otherwise. An analogous formula to Newton's 2nd law of translational motion and one that involves torque and rotational motion is $\Sigma\tau = I\alpha$. This is Newton's 2nd law for rotation. It shows that the rotational equivalent of force, torque τ, is equal to the moment of inertia, I, multiplied by the rotational acceleration, α. Similarly, instead of the translational kinetic energy equation of $K = \frac{1}{2}mv^2$, the kinetic energy of a rotating body, is equal to $K = \frac{1}{2}I\omega^2$. Moment of inertia is the rotational equivalent to mass, derived from the mass, shape, and axis of rotation of a body.

The shape of flywheels are often solid or hollow cylinders which range from a disc shape to a long drum [2]. The rotor geometry can be accommodated by the shape factor K. It is dependent on the polar moment of inertia and typically ranges between 0.3 and 1.0. It is associated with the efficiency of the system because when 100% of the specific energy

from the rotor material can be converted to specific energy from the shape and mass, K is equal to 1 [24]. A few values of K for common flywheel shapes are shown in Figure 4 [2].

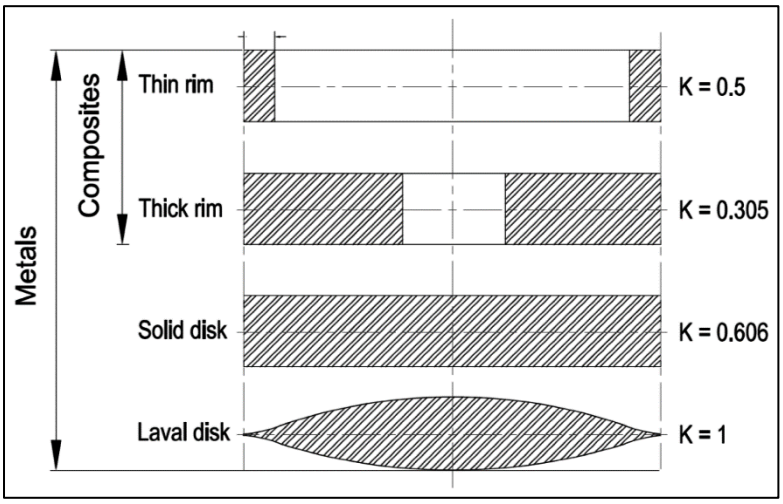

Figure 4. Shape factors, K, for different flywheel geometries

Since the rotor will be a hollow cylinder, the moment of inertia is $I = kmr^2$ [25]. K is the shape factor, m is the mass of the rotor, and r is the radius of the rotor. The shape factor, K, can be determined by using Figure 4, but it must first be determined if the wall is thick or thin. A wall is considered thin if its thickness is less than $\frac{1}{20}$ of the cylinder's diameter [26]. Table 1 shows a breakdown of determining K based on if the rotor wall is thick or thin. The middle row is the actual FESS used while the bottom row is an example of what the moment of inertia equation would be if the wall of the FESS were thin.

Wall thickness (in)	Diameter (in)	$\frac{1}{2}d$	Thick or thin?	Shape factor, K	Moment of inertia equation
0.5	3	0.15	Thick 0.5 > 0.15	0.305	$I = 0.305mr^2$
0.1	3	0.15	Thin 0.1 < 0.15	0.5	$I = 0.5mr^2$

Table 1. Determining moment of inertia equation based on wall thickness and shape factor, K

Based on Table 1, the moment of inertia equation is $I = 0.305mr^2$. This makes the kinetic energy equation stored in the thick-walled FESS $K = 0.1525mr^2\omega^2$. This forms the basis for the concept of an inertial energy storage system. It also proves that the stored energy of a flywheel can be increased either by having a higher moment of inertia or a higher speed [27, p. 7].

2.2 Flywheel Components

A FESS consists of a rotor, motor-generator, bearings, power electronics such as a charge controller and an electronic speed controller, a spindle or a shaft, and housing. Figure 5 is a schematic that shows the manufactured FESS and its components which is used in Chapter **Error! Reference source not found.** Experiment [2]. This model is like current FESS's on the market.

Figure 5. Components of the FESS

2.2.1 Power Electronics

The energy conversion from the source is accomplished by the motor-generator and a bi-directional power converter. A bidirectional converter allows power flow in both forward and reverse directions. This is important for FESS applications since the power flows in both directions when the flywheel is charging and discharging. A schematic showing the power flow of a typical FESS is shown in Figure 6 below [28].

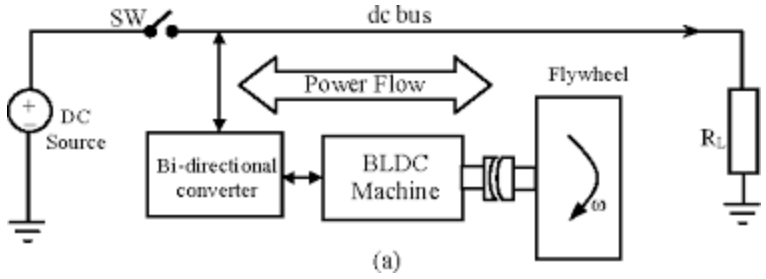

Figure 6. Power flow schematic of a typical FESS

As shown in the figure, the bi-directional converter and the brushless DC (BLDC) motor controls the energy flow to and from the flywheel [28]. A frequently used configuration for this specific application is the back-to-back (BTB) or AC-DC-AC connected to a DC link capacitor [2]. The topology of a grid-connected flywheel with a BTB converter in shown in Figure 7 [29].

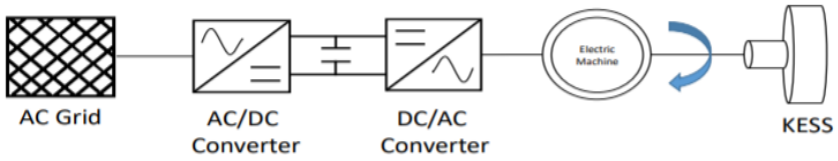

Figure 7. A grid-connected flywheel showing the BTB topology

The converters in this configuration are often controlled by the pulse width modulation (PWM) or the maximum power point tracking (MPPT) technique which modulates the width of its rectangular pulses to produce a variable wave form. The grid-side converter (AC/DC converter in Figure 7) converts the AC voltage to DC. Then the machine-side converter produces a sinusoidal AC current from a DC input {[2],[29]}. Based on the funds of this project, a bidirectional converter was not incorporated, and so power is only flowing in one direction in this case.

A solar charge controller with MPPT extracts the maximum energy from solar panels. The MPPT is designed to accommodate to weather changes to achieve optimal power [30]. A PWM charge controller maintains a constant voltage battery charging [31]. So, the MPPT charge controller always wants to achieve the maximum power, while the PWM charge controller keeps a constants charge. The PWM charge controller is cost effective and compact which are the reasons it was chosen instead of an MPPT charge controller for the FESS in this paper.

In a PWM charge controller, the current from the solar panel changes depending on the battery's condition and recharging needs. When the battery voltage reaches the regulation set point, the PWM slowly reduces the charging current to avoid overheating the battery. The voltage modulation is done by PWM control. The current from the charge controller will vary with the irradiance of the sun. The variance in current is not as crucial as it only effects the charge rate and not the maximum attainable speed of the flywheel. Power will flow only into the motor or the system load which would be a residential home in this case. No power generated from the flywheel will go through the charge controller. Power will flow from the charge controller until the solar panel drops below the system voltage of 24 volts. At which point, the voltage will not be high enough to power the system load. The solar charge controller chosen for this FESS is shown in Figure 8 along with a wiring diagram for connecting it to a home with solar panels [32].

Figure 8. Y-Solar charge controller

This is not to be confused with the FESS setup for this research which is shown below.

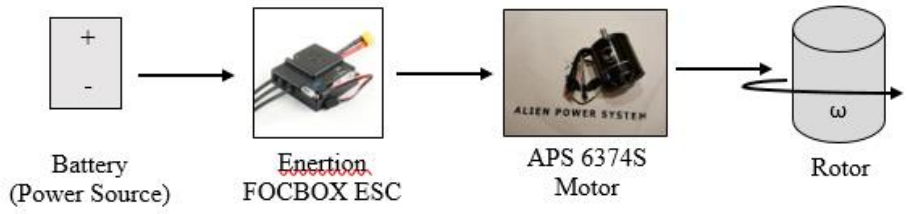

Figure 9. Power flow of manufactured FESS setup

Aside from the solar charge controller, a speed controller manages the speed of the rotor by controlling how much energy the motor is consuming, when the battery gets charged and discharged, and it tracks the energy being drawn out of the system. A FOCBOX Vedder electronic speed controller (VESC) made by Enertion was chosen as the speed controller. It is an open-source programmable controller that reads the incoming voltage and current

to keep the system load at its desired power level. This balancing will be done through charge and discharge of the stored energy. The VESC consists of a microcontroller, mosfets, and motor drivers. It can be programmed with C language through its USB port. Benjamin Vedder, a Swedish engineer, developed the open-source VESC Tool that was used for this FESS. The tool can configure VESCs, update VESC firmware, and generate real time data [33]. A snapshot of the VESC Tool generating real time data is shown in Figure 10.

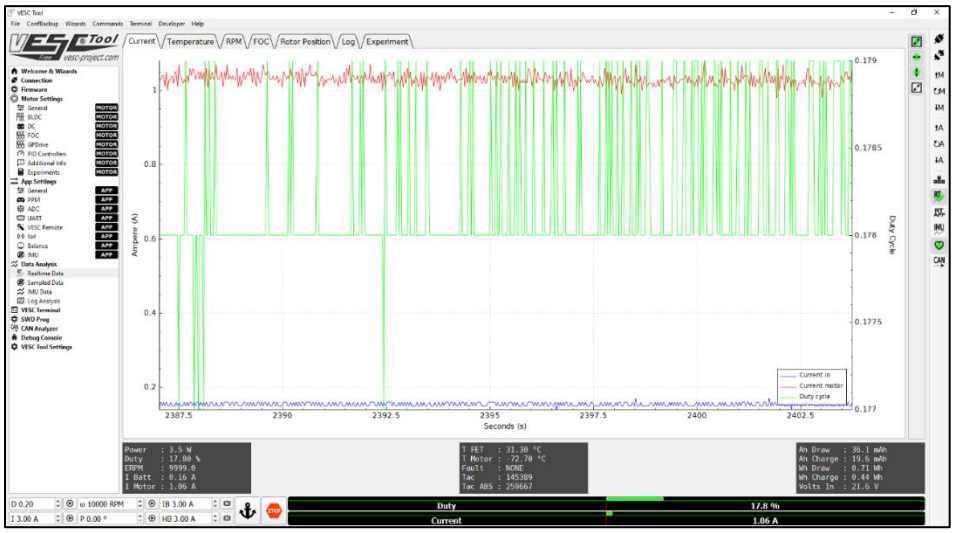

Figure 10. VESC Tool

The motor will be driven by the VESC using PWM control as it is a 3-phase drive. Power generation from the flywheel will be done through regenerative braking which is essentially reverse PWM control. The VESC has a max continuous current rating of 60 amps and can run up to 33.6 volts. The VESC will control the motor through its sensors up to 11,000 revolutions per minute (RPM). The VESC that is being used for this FESS is shown in Figure 11 [34].

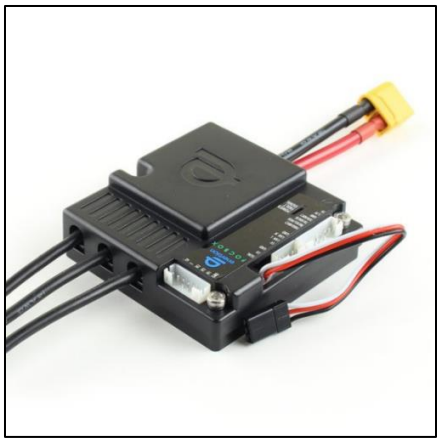

Figure 11. Enertion FOCBOX ESC

2.2.2 Motor-generator

The electric machine of the system must be a motor-generator which will be coupled to the flywheel to enable the energy conversion and charging of the flywheel. The flywheel charges when the motor-generator acts as a motor and beings to accelerate the flywheel by drawing energy from the electric source. The flywheel is discharged using the same electric machine, but this time it is acting as a generator and slows down the flywheel as it discharges [2].

Electric motors fall into two main categories, AC and DC machines. AC machines operate on alternating current where DC machines operate on direct current. Common AC machines used are induction machines (IM) and permanent magnet machines (PM). Induction machines are used for high power applications because of its ruggedness, high torque, and low cost. They have many attractive features such as simplicity, high reliability, wide speed range, and low maintenance [35]. They are commonly used for wind turbine

applications since IMs can smooth the power of wind generation systems. For FESSs, PM machines are mainly used because of its high efficiency, high power density, and low rotor losses. The issues with PMs are its high price, low tensile strength, and its idling losses due to stator eddy current losses [2]. When a PM motor is running at ultra-high speeds, its tensile strength is not high enough to withstand the large centrifugal tension caused by rotation [36]. This limits the RPM of the motor. PMs generate what is known as eddy current losses, they can be undesirable for electrical machines such as FESS because eddy currents generate thermal heat which causes losses {[37], [38]}. A massive conducting body that is subjected to a time-varying magnetic field. Voltages are induced in the body, which causes currents to circulate in paths. The currents are distributed and are called eddy currents [39].

DC motors can be either brushed or brushless. Brushed motors are low cost, low efficiency, low range of speeds, and high maintenance. A brushless DC motor is actually a PM AC motor where instead of commutating through brushes, electronic commutating is used [40]. Brushless motors have a high initial cost, high efficiency, high range of speeds, and require little to no maintenance. Due to the high efficiency and speed range, brushless motors present a large advantage for a solar panel and flywheel system. Motor selection is determined by the RPM, torque and power necessary for the system. The motor selected for this flywheel is the Alien Power System (APS) 6347S Sensored Outrunner Brushless Motor shown in Figure 12 [41]. This motor was chosen based on the moment of inertia and

Figure 12. APS 6374S Sensored Outrunner Brushless Motor

motor constants. From those values, the maximum RPM, stall torque and peak power can be calculated. All of these values along with the cost and size of the motor were the deciding factors.

2.2.3 Rotor and Spindle

The maximum speed at which a flywheel can operate is determined by the tensile strength of the rotor material. The stress experienced by the rotor must be kept below the strength of the rotor material to keep a suitable safety margin. The maximum stress of a thin rotating disc is explained by Equation 1 [2].

$$\sigma_{max} = \rho r^2 \omega^2$$

Equation 1. Maximum stress of rotor

In Equation 1, σ_{max} is the maximum stress, ρ is the density of the flywheel material in kilograms per cubic meter $\left(\frac{kg}{cm^3}\right)$, ω is the angular velocity in radians per second $\left(\frac{rad}{s}\right)$, and r is the outer radius in meters. This equation changes depending on the rotor geometry,

but the maximum stress is always proportional to the density and the square of the peripheral speed rw.

High speed flywheels, around 100,000 RPM, typically have a lighter rotor material while low speed flywheels, around 10,000 RPM, have a heavier rotor material. A disadvantage of high speed flywheels are that they are more expensive than a low speed flywheel since they are typically made with a much more expensive rotor material such as carbon fiber composites and typically require magnetic bearings [2]. Due to the ability of high-speed flywheels being able to reach higher speeds, the size of the unit can be smaller than a low speed flywheel unit due to its ability to generate more energy. This is an advantage especially when space is limited. An advantage of low speed flywheels are its low cost and ease of manufacturing. A disadvantage of low speed flywheels are that they suffer from idling losses when the flywheel is not in use [42]. The material of the rotor and spindle is important to ensure the design does not succumb to creep or fatigue and fail before intended [43]. The two commonly used materials for the rotor are solid steel or a composite material such as carbon fiber.

The spindle is driven by the motor which allows the rotor to spin. For the spindle, steel was chosen because of cost and availability. Facing was done on the spindle to make a square spline that allowed the rotor to be hard mounted to it. A jaw-type flex coupling was chosen as the connection between the motor shaft and the spindle since it provides tolerance for shaft misalignment. This tolerance reduces vibration, wear on bearings and other

mechanical problems caused by misalignment. For this FESS, a three-inch outer diameter (OD) and a two-inch inner diameter (ID) and four-inch height steel rotor was chosen primarily because of cost and manufacturing. A close-up of the rotor and spindle is shown in Figure 13.

2.2.4 Bearings

The bearing system of a FESS can be mechanical or magnetic depending on the weight, lifecycle, and losses associated with the flywheel. Mechanical ball bearings have traditionally been used, but these have higher frictional losses and require more maintenance due to lubricant deterioration. These problems can be alleviated by using a hybrid system of both mechanical and magnetic bearings. A magnetic bearing has no friction losses and does not need any lubrication. A mechanical bearing can stabilize a flywheel by keeping it vertically aligned. This can suppress the rotor vibrations in the vertical direction.

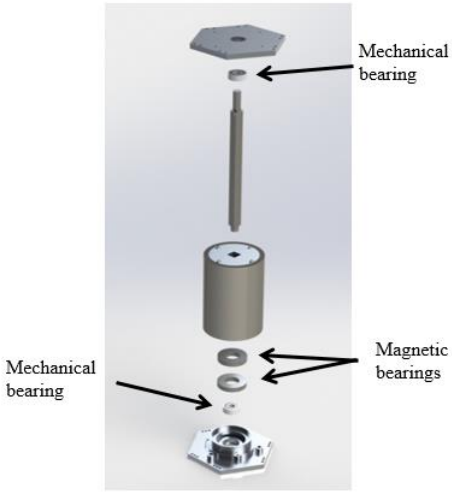

Figure 13. Close-up of inside of FESS

Due to the benefits of a hybrid system, both mechanical and magnetic bearings are included in the FESS. Figure 13 points out the magnetic bearings where one is attached to the bottom of the rotor using adhesive and the other is inserted to the bottom plate. The mechanical bearings are hard mounted into the top and bottom plates as shown in Figure 13. The bottom mechanical bearing is hard mounted underneath the bottom magnetic bearing.

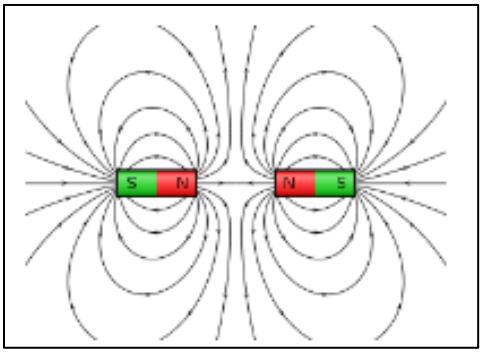

Figure 14. Magnetic fields of two cylindrical magnets oriented to repel each other

Magnetic bearings allow for contact free rotation of an object through the attractive or repulsive magnetic forces. Shown in Figure 14 are the opposing repelling fields of two cylindrical bar magnets [44].

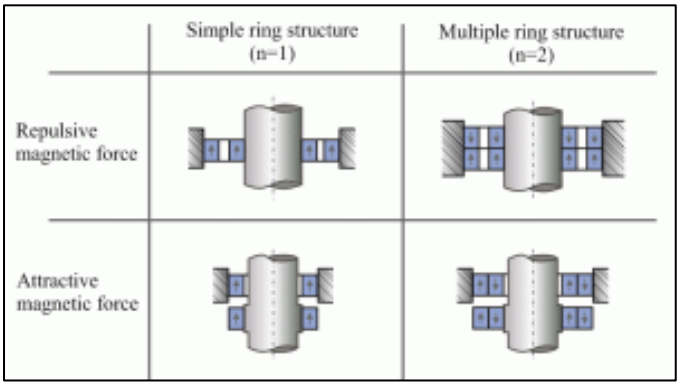

Figure 15. Various magnetic bearing configurations

Magnets can be oriented in a number of ways to act as a magnetic bearing, as shown in Figure 15 [44]. Depending on the design and orientation of the magnets, it is possible to stabilize the rotating object's radial, axial, and tilt directions. Large scale flywheels may involve active magnetic bearings, which use electromagnets to suspend the rotating mass. Permanent magnet bearings (PMB), also known as passive magnetic bearings, has benefits such as they do not need actuators, coils or power electronics, making them cheap, small, and simple. One of the major drawbacks to PMBs is the lack of damping. They cannot minutely control all degrees of freedom at the same time, thus require additional means to create reasonable stability. The effects of vibrations caused by unbalance, slight magnetic tolerances, and external excitations can be lessened with damping measures [45].

The force the magnetic bearing would produce needs to be calculated to make sure it is able to hold up the weight of the rotor. This value had to be slightly larger than the weight of the rotor, but not large enough to cause the rotor to push itself into the top plate. The manufacturer of the magnetic bearings used in the FESS system, K&J Magnetics, has an online calculator that calculates the force of the magnets needed to hold up a specific weight. Using this calculator, two magnets repelling each other with a two-inch outer diameter, one-inch inner diameter and one quarter of an inch thickness was needed for the specific rotor used in the FESS.

2.2.5 Housing

The housing creates an area with less drag and houses the flywheel in case of a failure. The drag losses can be reduced by mounting the flywheel in a vacuum enclosure to improve the performance and safety of the system. Vacuum chambers can cost between hundreds and thousands of dollars, but are very attractive to use in FESS's due to their ability to reduce drag losses [46]. The housing holds the rotor in the vacuum to control the drag losses by maintaining the low pressures within the housing. A vacuum pump is required to maintain the heat generated by the motor-generator, and possibly other components within the housing [2]. For this FESS, a vacuum enclosure will not be used. This information is just to give a brief background of the most common components in a FESS.

If a failure were to occur, composite rotors tend to break into many small fragments that rotate inside the casing. Due to this, pressure builds up within the housing. If air were to enter during this, a dust explosion can occur. Steel rotors can break into several pieces which can be hard for the housing to withstand. Therefore, large housing systems must be used for solid steel rotors. For this FESS, a smaller housing system with two walls was used since cost and size were constraints. The mode of failure expected of the rotor design is its stress reaching higher than its ultimate tensile strength. Therefore, causing the rotor to rupture.

Housing material and construction is of critical concern for strength, weight, and safety of the FESS. Due to the machinability of aluminum, it is an ideal material for a motor mount,

top plate, and bottom plate components. The shatter guard will need to be constructed to prevent the flywheel mass from puncturing the housing in the event of a failure. The housing is usually made out of thick steel or another high strength material such as composites [47]. The shatter guard and square brace are shown in Figure 16. Since cost and size were limiting factors, a smaller housing with two walls was chosen. An aluminum square brace was chosen not only to protect the rotor from exploding out of the case, but to keep the alignment of the entire system. Each seam created by the square brace is covered by the shatter guard so that there are open areas for the rotor the puncture through.

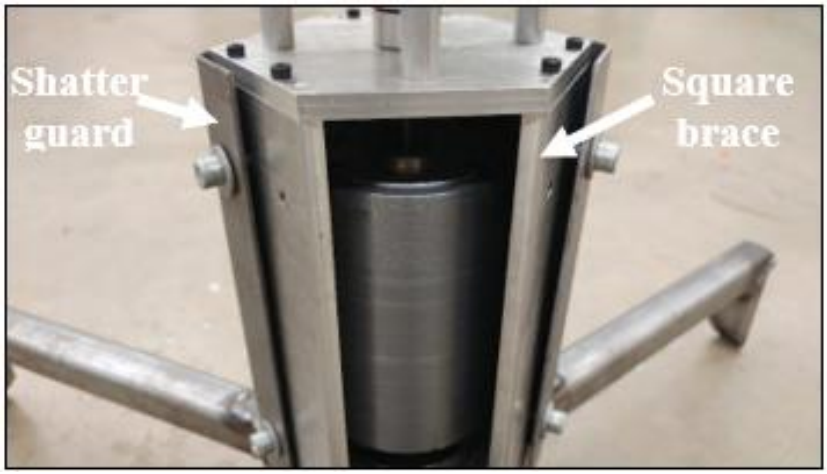

Figure 16. Shatter guard and square brace

Figure 17 shows the entire FESS with the motor cap and fan. For safety reasons, the motor is encased in a 3D printed motor cap. There is a chance the motor will overheat since it is enclosed, so a fan is screwed onto the top of the motor cap to increase airflow.

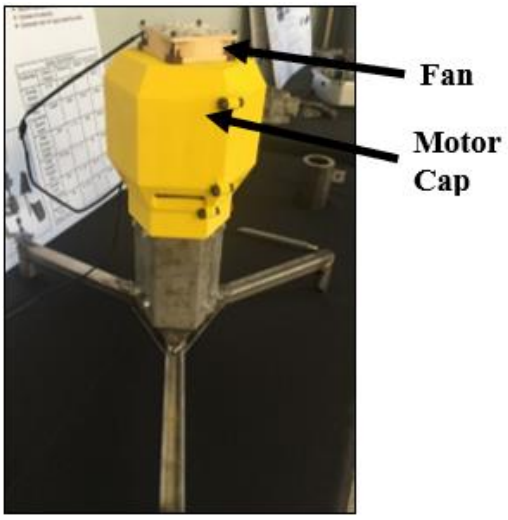

Figure 17. FESS with motor cap and fan

An important safety factor about FESS's are that they are installed in the ground and are typically surrounded by concrete. Installing a FESS underground protects the surrounding environment and people in the event the FESS was to fail. Beacon Power, an American company that specializes in flywheel-based energy storage, puts their systems inside of a three-piece, pre-cast concrete foundation. This is shown in Figure 18 [48].

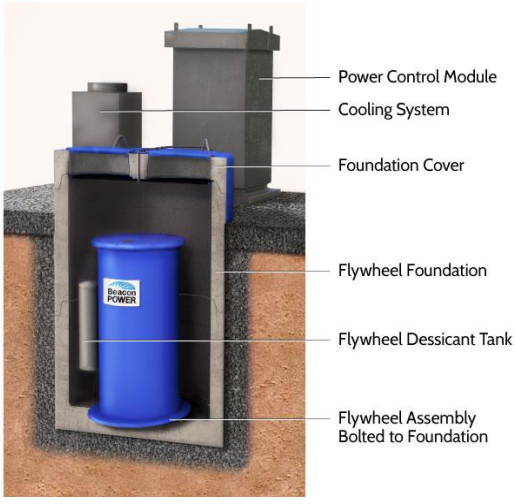

Figure 18. Beacon Power System Installation

Amber Kinetics also installs their M32 flywheels underground as a safety precaution. The flywheel is placed inside of a capsule that is surrounded by highly compacted soil. This is shown in Figure 19 [49].

Figure 19. Amber Kinetics System Installation

CHAPTER 3

Experiment

The experimental setup described in Chapter **Error! Reference source not found.** will be used to perform speed tests and observations. A breakdown of the FESS is shown in Table 2. To power this experimental setup, two lithium polymer (LiPo) batteries connected in series were used. In the actual setup, a 24-volt battery would be used. With this setup, I am simulating a system design for use in Sacramento. I am also going to observe the FESS to see how it responds to speeds in terms of system vibrations, speed data, and motor sounds. This is to see how the system currently acts.

Component	**Company/model**
Power Source	2 x SMC 3S 11.1V 1500mAh LiPo batteries
Motor	APS 6374S
ESC	Enertion FOCBOX VESC V1.7
Rotor	1026 Carbon Steel 3” OD x 2” ID x 4” Height
Bearings	2 x Boca Bearing SR6C-YUU TH9/C3 BK #5 NB2 2 x K&J RY0X04

Table 2. FESS Specifications

Theoretical calculations of the amount of power produced by the momentum of the rotor was calculated for the specific design in the table below. Based on the result, a larger scale of the original FESS design was introduced, FESS design #2, and the same power calculations were done. In addition, two FESS designs identical to the original FESS and

FESS design #2, were introduced except their rotors are made of the carbon fiber composite T1000G/epoxy.

All four of these FESS designs will be tested to see if they can reach the target goal of 10,000 kWh which is the annual energy consumption of a house in Sacramento according to the SMUD. This is about 27 kWh daily. As mentioned in Section 2.2.3 Rotor and Spindle, the tensile strength of the material determines the maximum speed of the flywheel. With every speed that is tested, the maximum stress of the rotor is calculated using Equation 1. The speed of the FESS is measured using the VESC tool mentioned in

2.2.1 Power Electronics. This tool is important in controlling the speed of the motor, updating the VESC firmware and programming the VESC.

As mentioned in Section

2.2.5 Housing, since commercial FESS's are installed underground and the FESS used for this experiment is not installed underground, the maximum speed will not be tested. Rather, speeds were tested until a significant change occurred in the graphs that indicated unsafe speeds. This will be later discussed in Chapter **Error! Reference source not found.**. These speed tests were done to determine if the original FESS design will have to be installed underground due to a change in the RPM plots.

3 Although the results will be in RPM, the VESC tool originally outputs the speed with the unit ERPM which is the electrical RPM. The relationship between ERPM and RPM has

to do with the number of pole pairs in the motor. Mechanical RPM is how many times the rotor can make a full revolution and return to its original position within a minute. Electrical RPM is how many times the motor completes a full revolution with one polarity change. A two-pole motor completes a full revolution with one polarity change whereas a four-pole motor only has to rotate 180° with one polarity switch [50]. Therefore, the calculation between ERPM and RPM is simply dividing the ERPM by the number of pole pairs in the motor. The VESC tool generates the speed with a unit of ERPM since the VESC tool does not know the exact construction of the motor [51]. Since ERPM is the unit used by the VESC tool, this is the unit that will be used in these results. The energy of the original FESS design is calculated using **Error! Reference source not found.**. A breakdown of all of the equations used and in what order they are used is shown below in Section 3.1 Equations.

4.1 Equations

First step is to approximate the radius, r, in meters since the rotor of the FESS is a hollow cylinder as shown in Figure 20. This is done by taking the average of the outer and inner

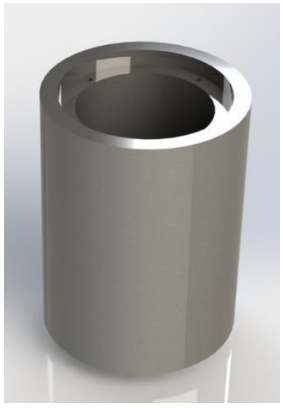

Figure 20. Rotor design

radius, r_o and r_i respectively, as shown below. Next step is to calculate the kinetic energy in joules by

$$r = \frac{r_o + r_i}{2}$$

Equation 2. Approximation of the radius of a hollow cylinder

using $K = 0.1525mr^2\omega^2$ as described in Section 2.1. M is the mass of the rotor in kilograms, r is the radius of the rotor in meters, and ω is the angular velocity in radians per second.

The maximum stress must also be calculated to determine if it is exceeding the tensile strength of the rotor material which is AISI 1026 carbon steel. The maximum stress will be calculated using Equation 1: $\sigma_{max} = \rho r^2 \omega^2$. The tensile strength of AISI 1026 carbon steel is 71,100 psi (490 MPa) and its density is 7858 $\frac{kg}{m^3}$ {[52], [53]}. As mentioned, before each speed is tested using the VESC tool, the maximum stress is calculated to make sure it does not go above the ultimate tensile strength. Otherwise, the rotor will

rupture. Figure 21 shows the experiment setup of the original FESS which is isolated from the batteries and the computer that is running the VESC tool for the data collection. The FESS is isolated for safety reasons in the event the rotor is to fail.

Figure 21. FESS experiment setup

4.2 Software and Hardware Summary

The software used to run the speed tests is the VESC tool described in 2.2.1 Power Electronics. This program was used on a Windows 10 computer and was connected to the system as shown in Figure 22 below. The ESC is connected to the computer via a USB

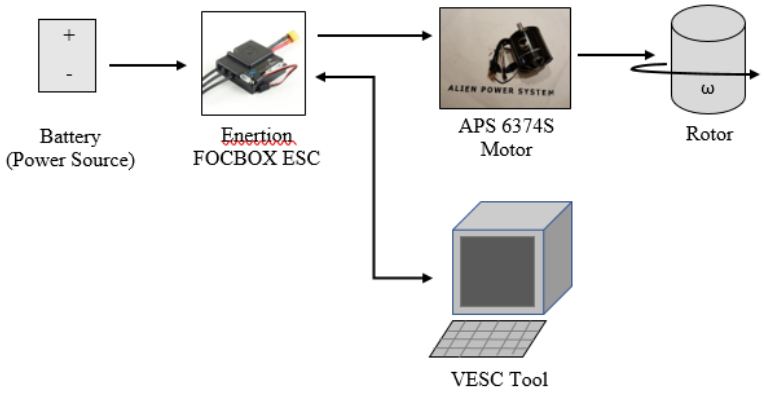

Figure 22. Software and hardware setup

cable and allows the user to control the speed of the motor using the VESC tool. Once a speed is chosen, real-time speed data is generated and can be exported to examine at a later time.

4.3 VESC Tool Parameters

The VESC tool can generate real-time data that allows users to understand how to set up their VESC's and motors. This real-time data function was used to observe how the original FESS motor reacted to certain speeds. To run the speed tests, speeds were chosen for the motor to spin up to and stay at that speed for about 10 seconds. After 10 seconds, the motor was stopped using the full brake button. Although the VESC tool outputs the speed in ERPM, RPM is desired as the unit for clarity reasons. As mentioned in

2.2.1 Power Electronics, the ERPM is the electrical RPM and when divided by seven, the number of poles in the motor, is converted to RPM.

CHAPTER 4

Results and Analysis

5.1 VESC Tool Results

Speeds tested below 7,000 RPM all had an overshoot at startup. The overshoot is a similarity between each speed, which is shown when comparing 5,714 RPM, shown in Figure 23, and 7,000 RPM, shown in Figure 24. When the motor first starts and begins spinning up to the designated speed, it overshoots pass the designated speed, then slows and levels out at that designated speed. The motor continues to stay at that speed until the user initiates a brake, or in this case, a full brake where the motor uses all its power to stop spinning.

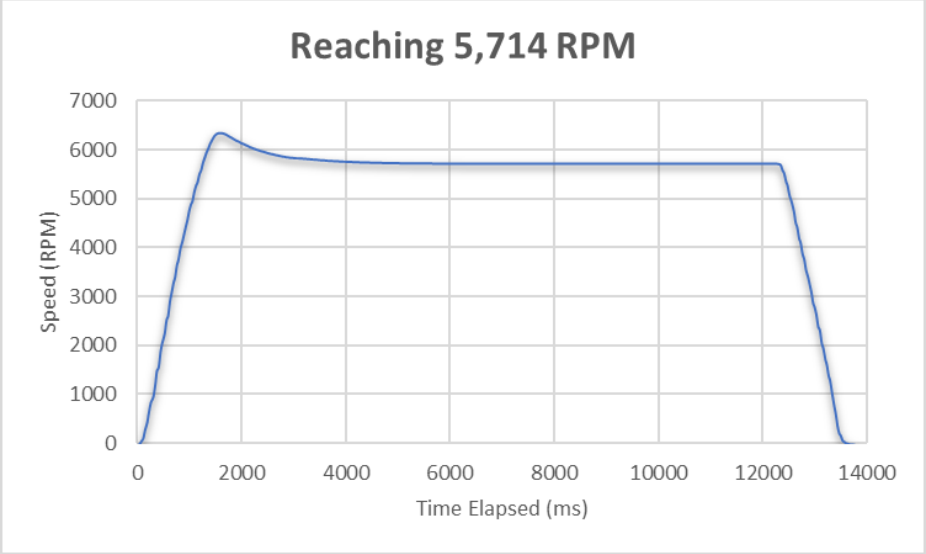

Figure 23. Reaching 5,714 RPM

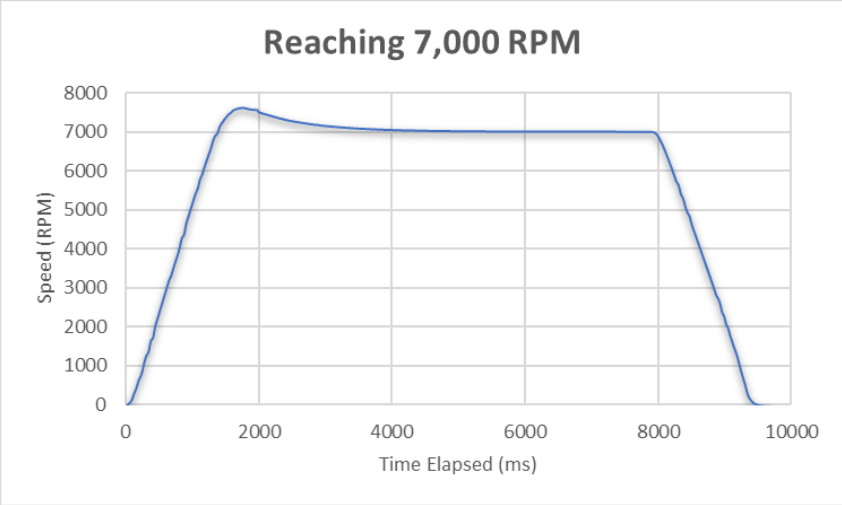

Figure 24. Reaching 7,000 RPM

A change in the RPM plots was found at 8,000 RPM where the overshoot no longer occurred. This is visible when comparing Figure 24 and Figure 25. The speed 8,000 RPM was determined as the stopping point for the speed test since the overshoot no longer appeared in the plots. All of the data for these plots are in Appendix A.

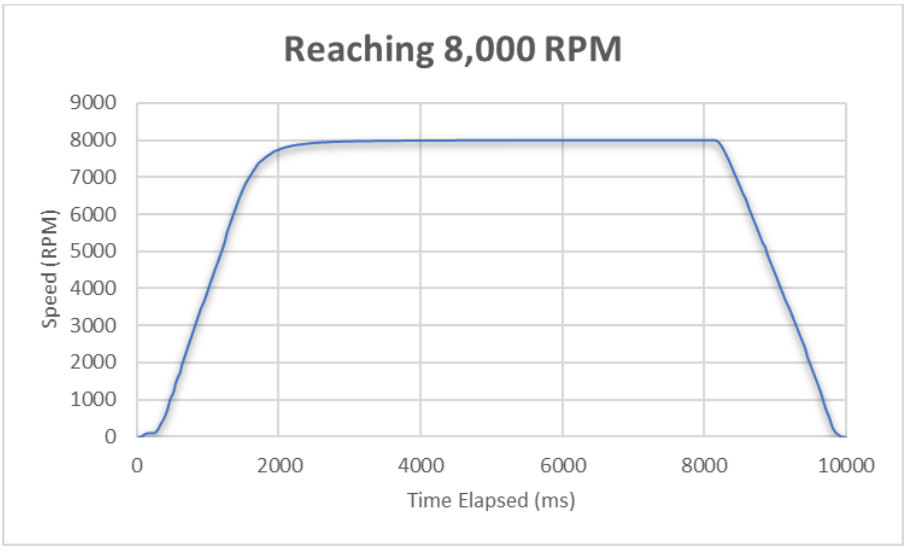

Figure 25. Reaching 8,000 RPM

5.2 Calculation Results and Discussion

Based on the original FESS design, theoretically, the rotor's maximum speed is about 53,106 RPM without the maximum stress exceeding the ultimate tensile strength of the material and with a safety factor of 2. The original FESS design would be able to produce $1.15\ x\ 10^{-5}\ kWh$ per day which is significantly lower than the target energy production value of $27\ kWh$. Based on this result, a larger rotor is needed to reach the target value.

Since the original FESS design does not meet the energy demand value of 27 kWh daily, other configurations will be tested using their property values to see if they can meet the energy demand value. These configurations include a larger version of the original FESS design, a composite version of the original FESS design, and a larger composite version of the FESS design. A breakdown of the FESS designs is in Table 3 below. Natural frequency and critical speed are not included in the calculations due to their complexity regarding the FESS designs.

	Original FESS design	FESS design #2	FESS design #3	FESS design #4
Material	1026 Carbon Steel	1026 Carbon Steel	T1000G/epoxy	T1000G/epoxy
Inner Diameter (in)	2	36	2	36
Outer Diameter (in)	3	48	3	48
Height (in)	4	48	4	48

Table 3. FESS Configurations

The dimensions for FESS design #2 were chosen based on if it could produce a significant amount greater than the original FESS design without being too large. The dimensions of this design are shown in Table 3. The same calculations were done to FESS design #2 as those done to the original FESS design. FESS design #2 would, theoretically, be able to produce 0.212 kWh per day and have a maximum speed of 3,158 RPM. Again, this is without the maximum stress exceeding the ultimate tensile strength of the material and with a safety factor of 2.

Due to the increased size of this design, it was determined not feasible to have an individual FESS for a residential house in Sacramento. As a result, another route of how to go about reaching this energy demand value was introduced. Since the energy production value of FESS design #2 is much closer to the target energy production value, another calculation was done to see how many FESS's would be needed to reach the target value. About 129 flywheels would be needed to reach the $27\ kWh$ energy production value. Since flywheel energy storage companies, such as Beacon Power, create flywheel power plants with only 200 flywheels, this number of flywheels is reasonable [54]. As a result, another FESS design was introduced.

FESS design #3 uses the carbon fiber T1000G/epoxy composite because of its physical properties and lightweight. Its high tensile strength, low coefficient of thermal expansion (CTE), and its low density are all attractive qualities for an FESS rotor [55]. This specific carbon fiber is the world's highest tensile strength carbon fiber [56]. These qualities can

decrease the overall size of a FESS due to the materials ability to reach higher speeds. Composite materials are capable of rotating at 10,000 to 100,000 RPM without fracturing and are capable of storing more energy due to these high speeds [57]. This was chosen as the angular velocity speed range for both FESS design #3 and FESS design #4.

As shown in Table 3, FESS design #3 is the same size as the original FESS design. The size of FESS design #3 was chosen to be the same as the original FESS design so that the energy production can be compared between the two. Since this design is a different material, the shape factor, K, is also different. The shape factor is 0.9647 and will change the kinetic energy equation from $K = 0.1525mr^2\omega^2$ to Equation 3 [58].

$$K = 0.4824mr^2\omega^2$$

Equation 3. Kinetic energy stored in T1000G/epoxy FESS

FESS design #3 would, theoretically, be able to produce $1.38\ x\ 10^{-5}\ kWh$ per day at 100,000 RPM while also being well under the maximum stress limit.

FESS design #4 is also designed to be made out of T1000G/epoxy composite, but at the same size as FESS design #2, as shown in Table 3, to compare the energy production differences between 1026 carbon steel and T1000G/epoxy. At this size, the FESS can theoretically produce $2.74\ kWh$ per day while spinning at about 29,208 RPM. This is without the maximum stress exceeding the ultimate tensile strength of the material. The number of flywheels needed to reach the target value was calculated since the energy production value is close to the target value. Ten of these FESS's would be needed to

reach 27 kWh which is very reasonable since current flywheel power plants have around 200 FESS's.

	Original FESS design	FESS design #2	FESS design #3	FESS design #4
Material	1026 Carbon Steel	1026 Carbon Steel	T1000G/epoxy	T1000G/epoxy
Maximum Speed (RPM)	53,106	3,159	100,000	29,208
Energy Produced (kWh per day)	$1.15\ x\ 10^{-5}$	0.21	$1.38\ x\ 10^{-5}$	2.74
Number of FESS Needed to Reach Target Value	2,381,439	129	1,990,692	10

Table 4. Comparison of FESS Design

A comparison of all the FESS designs is shown in Table 4. All of the calculations are shown in Appendix B. Comparing the original FESS design to FESS design #3, the latter produces slightly more energy which means less FESS's are needed. This can be explained by the ability of T1000G/epoxy to reach much higher speeds without experiencing stresses higher than the ultimate tensile strength. At the indicated speeds in Table 4, the original FESS design reached half its maximum stress limit whereas FESS design #3 was well under its maximum stress limit. Due to this, the rotor at its original size of 2" ID, 3" OD, and 4" height would be best made of T1000G/epoxy than 1026 carbon steel. This design, even if the rotor is made of T1000G/epoxy, is not able to produce enough energy and would take millions of FESS's to reach the desired energy production value.

Both FESS design #2 and FESS design #4 can reach the energy production demand of 27 kWh with a reasonable amount of FESS's. An advantage of FESS design #2 is that it would be cheaper in cost since it is made of 1026 carbon steel rather than a composite material. Composites are known for being expensive whereas in comparison, steel is inexpensive. A disadvantage of FESS design #2 is that 129 FESS's are needed whereas for FESS design #4 only 10 FESS's are needed. Determining which design is appropriate depends on if cost or number of FESS's wants to be kept to a minimum. Both designs have some drawbacks, but they show great potential in achieving the energy production value.

Comparing all of the FESS designs, it is apparent that the larger designs show much more promise of achieving the energy production demand. Even though the larger designs show more promise, one FESS is not enough to supply all of the energy needed. It is also apparent that FESS design #4 has the most potential due to its energy production value and the number of FESS needed to reach the energy production demand.

5.3 FESS Specifications

After comparing all four of the FESS designs, FESS design #4 would be the best option in cases where cost is not important, while FESS design #2 would be the best option where cost is important. FESS design #4 requires significantly less flywheel units which is an advantage especially if space is limited. Both designs can reach the energy

production value with a reasonable amount of FESS's and both are plausible designs. Table 5 shows a side-by-side comparison of these FESS designs.

	Material	Maximum Speed (RPM)	Energy Produced (kWh per day)	Number of FESS Needed to Reach Target Value
FESS design #2	1026 Carbon Steel	3,159	0.21	129
FESS design #4	T1000G/epoxy	29,208	2.74	10

Table 5. FESS design #2 and FESS design #4

I was not able to meet the energy production value of 10,000 kWh with the original FESS design due to its small size and rotor material having a relatively low ultimate tensile strength in comparison to carbon fiber. In terms of meeting the energy production value, I have succeeded in achieving this goal through FESS designs #2 and #4. I have failed in terms of having a single unit be able to reach the energy production value since all designs need multiple units to reach this value.

CHAPTER 5

Conclusion

FESS's are a great alternative for storing excess energy produced by houses. Based on the energy consumption of an average house in Sacramento, FESS design #2 and FESS design #4 are both adequate means of fulfilling the energy demand of 27 kWh daily. Both designs have the dimensions 36" ID by 48" OD by 48" in height. Although, both designs will need their own flywheel power plants to completely fulfill the energy production demand. These FESS's were designed to be integrated with a solar panel. The excess energy from the solar panel that is not being used by the residential house, would be put towards charging the FESS.

The effectiveness of a FESS system in a specific city is dependent on a variable called the energy consumption value. This variable is easily interchangeable and allows for straightforward calculations on whether the city would benefit from a FESS system. In this research, Sacramento was chosen as the city and the energy production value was calculated to determine whether the city would benefit from it. This research can be used for any city so long as the energy consumption value is changed to reflect the chosen city. There may be some cases in which opting for a larger FESS unit, such as Amber Kinetics M32 flywheel, would be better than a large quantity of either FESS design #2 or #4. This is primarily due to a scaling issue of price, where in order to meet the energy consumption value you may not only exceed the cost of the larger FESS unit, but also end up using more space.

CHAPTER 6

Future Considerations

Of interest is the critical speed of the FESS designs that have been described. The critical speed is the rotational speed at which forces cause a machine component to vibrate at its natural frequency and can cause the entire machine to experience resonant vibrations [59]. Both the critical speed and the maximum stress experienced by the flywheel determines the maximum speed of the FESS.

Also, of interest is using or designing higher strength and lower density materials since they can store more energy. Previously published studies have shown that a higher strength and lower density composite is needed in order to obtain higher energy densities [58]. A material that can produce enough energy to support the energy demand of a house not only in Sacramento, but in other cities is worth looking in to. Each individual unit will not affect the other units since they are not interconnected at a flywheel power plant.

FESS's have been used in flywheel power plants that create multiple megawatts of power for balancing frequency regulation. Smaller scale FESS designs involve smaller microgrids such as a parking garage and server room [60]. A FESS designed for a case in between, such as for a tiny house, would reduce the number of solar panels some tiny houses have for high power usage. This would also reduce unsustainable energy and would work well in tandem with solar panels.

APPENDIX A

5,714 RPM Data

Time (ms)	RPM
0	-37.1429
31	-36.7143
81	39.14286
119	108.2857
149	267.7143
191	421.2857
227	648.2857
261	827.1429
307	945.7143
344	1187.143
377	1475.143
411	1554
445	1854.714
478	2043.714
524	2232
561	2514.857
594	2612.857
627	2895.714
661	3083.714
694	3273.429
725	3393.286
761	3639.143
791	3753
828	3982.143
867	4128.143
899	4282.429
930	4424.286
961	4558.286
994	4740.429
1028	4878.571
1060	4957.286
1094	5139.143
1127	5264
1158	5343
1194	5504.571429
1224	5578.714286
1260	5731.428571
1293	5839.714286
1328	5946.428571
1369	6043
1399	6127.428571
1486	6291.142857
1546	6336.571429
1587	6344.285714
1617	6343
1647	6336.285714
1679	6324.714286
1709	6310.428571
1744	6286.714286
1774	6268.142857
1804	6250.142857
1835	6230.428571
1906	6186.285714
1931	6177
1962	6159.428571
1994	6136.428571
2027	6126.428571
2060	6110.142857
2093	6093.142857
2126	6078
2161	6055
2191	6046
2228	6027.428571
2258	6019
2294	6001.857143
2325	5994
2361	5978.142857
2399	5968.142857
2431	5958
2461	5948.714286
2494	5936.142857
2527	5926.714286
2560	5917.571429
2593	5913
2624	5903.428571
2660	5892.142857
2691	5887.142857
2728	5876.857143
2758	5872.428571
2794	5862.857143
2825	5859
2861	5850.714286
2898	5846.142857
2928	5841.285714
2962	5836.571429
2993	5833.571429
3026	5831.285714
3061	5828.428571
3094	5827.428571
3127	5825.571429
3158	5823.142857
3194	5819.714286
3224	5818
3261	5814.142857
3291	5812.142857
3327	5807.857143
3365	5805.142857
3400	5801.857143

3429	5799
3460	5796
3494	5792.142857
3527	5789
3560	5786
3593	5784.857143
3624	5781.428571
3660	5777.857143
3694	5775.285714
3725	5773.857143
3760	5770.714286
3791	5769.285714
3828	5766.571429
3867	5764.714286
3898	5763
3928	5761.285714
3963	5759.428571
3994	5758
4027	5755.714286
4061	5754.142857
4093	5753.142857
4127	5751.714286
4158	5750
4194	5748.142857
4224	5747.285714
4260	5745.571429
4291	5744.714286
4328	5743.285714
4367	5742.142857
4398	5741.142857
4429	5740.142857
4461	5739.285714
4493	5738.142857
4528	5737.142857
4561	5736.285714
4593	5735.857143
4626	5735
4658	5734
4694	5733.142857

4724	5732.428571
4760	5731.142857
4791	5730.857143
4827	5729.857143
4866	5729.142857
4897	5728.714286
4930	5728.142857
4961	5727.571429
4994	5727.142857
5028	5726.714286
5061	5726.142857
5094	5725.571429
5125	5725.428571
5161	5724.571429
5192	5724.428571
5228	5723.857143
5258	5723.714286
5294	5723
5335	5722.571429
5366	5722.285714
5399	5722.142857
5431	5721.857143
5460	5721.571429
5493	5721.571429
5527	5721.285714
5561	5721
5593	5721
5626	5720.571429
5658	5720.428571
5694	5720
5724	5719.857143
5760	5719.714286
5791	5719.571429
5827	5719.142857
5868	5718.857143
5899	5718.857143
5928	5718.571429
5964	5718.428571
5993	5718.428571

6027	5718.285714
6060	5718.142857
6093	5718
6127	5717.857143
6158	5717.714286
6194	5717.714286
6224	5717.428571
6261	5717.142857
6291	5716.857143
6327	5716.857143
6365	5716.571429
6398	5716.571429
6431	5716.428571
6462	5716.142857
6493	5716.142857
6528	5716.142857
6560	5716
6593	5716
6628	5716
6658	5716
6694	5716
6724	5715.857143
6760	5715.857143
6791	5715.714286
6827	5715.714286
6869	5715.428571
6899	5715.428571
6930	5715.285714
6961	5715.285714
6995	5715.142857
7028	5715.142857
7060	5715.142857
7093	5715.142857
7127	5715.285714
7158	5715.285714
7194	5715.285714
7224	5715.285714
7260	5715.285714
7291	5715.285714

7327	5715.285714
7367	5715.142857
7398	5715.142857
7428	5715.142857
7461	5714.857143
7493	5714.857143
7527	5714.857143
7560	5714.857143
7593	5714.714286
7627	5714.857143
7658	5714.857143
7694	5715
7724	5715
7760	5715
7791	5714.857143
7827	5715
7865	5714.857143
7898	5714.857143
7932	5714.857143
7964	5714.857143
7993	5714.857143
8028	5714.857143
8061	5714.714286
8094	5714.714286
8125	5714.571429
8161	5714.428571
8191	5714.714286
8227	5714.714286
8258	5714.571429
8294	5714.714286
8336	5714.571429
8366	5714.428571
8398	5714.571429
8429	5714.571429
8461	5714.571429
8493	5714.571429
8527	5714.571429
8560	5714.571429
8593	5714.428571

8627	5714.428571
8658	5714.571429
8694	5714.428571
8724	5714.285714
8760	5714.428571
8791	5714.428571
8828	5714.428571
8868	5714.428571
8898	5714.571429
8929	5714.428571
8961	5714.571429
8993	5714.571429
9027	5714.571429
9060	5714.428571
9093	5714.571429
9124	5714.428571
9161	5714.428571
9191	5714.428571
9227	5714.428571
9258	5714.571429
9294	5714.428571
9325	5714.428571
9361	5714.571429
9399	5714.428571
9431	5714.285714
9460	5714.285714
9494	5714.285714
9527	5714.428571
9560	5714.285714
9593	5714.428571
9624	5714.428571
9660	5714.428571
9691	5714.428571
9727	5714.571429
9758	5714.428571
9794	5714.428571
9835	5714.428571
9867	5714.285714
9897	5714.285714

9929	5714.428571
9964	5714.142857
9993	5714.142857
10026	5714.142857
10060	5714.285714
10093	5714.428571
10126	5714.428571
10161	5714.285714
10191	5714.285714
10227	5714.285714
10258	5714.142857
10294	5714.285714
10324	5714.285714
10361	5714.142857
10397	5714.142857
10427	5714.142857
10460	5714.285714
10495	5714.428571
10527	5714.285714
10560	5714.285714
10593	5714.285714
10627	5714.428571
10658	5714.142857
10694	5714.285714
10724	5714.285714
10761	5714.428571
10791	5714.571429
10827	5714.571429
10866	5714.428571
10897	5714.428571
10932	5714.428571
10962	5714.428571
10994	5714.571429
11028	5714.428571
11060	5714.571429
11093	5714.428571
11128	5714.428571
11158	5714.428571
11195	5714.428571

11224	5714.285714
1261	5714.285714
11291	5714.285714
11327	5714.285714
11358	5714.285714
11397	5714.285714
11428	5714.285714
11474	5714.285714
11491	5714.285714
11528	5714.285714
11561	5714.285714
11593	5714.285714
11628	5714.285714
11658	5714.428571
11694	5714.571429
11725	5714.428571
11761	5714.571429
11791	5714.428571
11827	5714.285714
11858	5714.428571
11894	5714.428571
11931	5714.285714
11961	5714.285714
11994	5714.285714
12028	5714.285714
12061	5714.428571
12093	5714.285714
12127	5714.142857
12158	5714.428571
12207	5714.285714
12243	5714.285714
12277	5714.285714
12310	5708.857143
12344	5684.142857
12377	5580.857143
12408	5518.857143
12445	5350.857143
12474	5263.714286
12511	5065.142857

12542	4966.571429
12592	4754.714286
12627	4517.285714
12658	4413.714286
12694	4194.857143
12725	4091.571429
12760	3871
12791	3767.285714
12827	3542.142857
12866	3394.571429
12897	3246.142857
12928	3092.285714
12963	2871.285714
12993	2774.428571
13027	2619.285714
13060	2385.428571
13093	2310.285714
13128	2050.571429
13158	1942
13198	1715.714286
13225	1606.142857
13261	1379.857143
13291	1272.571429
13328	1012.714286
13368	757.8571429
13399	584.8571429
13431	356.4285714
13463	203.7142857
13494	153.7142857
13528	56.42857143
13561	26.28571429
13594	-0.714285714
13625	-10.28571429
13661	-24.14285714
13695	-29.85714286
13725	-29.71428571
13761	-33.14285714

7,000 RPM Data

Time (ms)	RPM
0	-39.1428571
44	25.57142857
91	120.4285714
117	260.8571429
157	417.7142857
194	627
240	804.1428571
277	1077.142857
310	1263
343	1359
377	1639.857143
410	1720.571429
443	2016.428571
477	2207.428571
509	2395.285714
543	2585
589	2843.428571
616	2994.714286
651	3193.714286
681	3301.714286
710	3471
743	3651.285714
776	3825
809	4020.857143
843	4274.857143
876	4363
909	4647.142857
943	4833.571429
976	5018.428571
1010	5201.857143
1043	5385
1087	5570.142857
1116	5780.142857
1148	5901
1177	6061.571429
1211	6238.571429
1243	6398.857143
1276	6555.857143
1310	6760.857143
1343	6894.714286
1376	6953.428571
1410	7121.857143
1443	7217.857143
1477	7302.571429
1510	7378
1543	7444.428571
1588	7502.714286
1616	7550.571429
1648	7572.285714
1678	7593.428571
1712	7607
1743	7611.428571
1776	7610.142857
1810	7598.857143
1881	7568.714286
1971	7558.142857
1995	7506.285714
2024	7488.142857
2056	7470.285714
2085	7453.428571
2117	7441.571429
2148	7424.714286
2179	7409.142857
2212	7392.571429
2243	7378.285714
2276	7363.571429
2309	7343.571429
2343	7336
2377	7316.428571
2411	7303.57
2443	7291.57
2477	7280
2510	7268.86
2544	7258
2588	7247.43
2617	7238.71
2650	7229.57
2680	7221.29
2713	7212.71
2743	7205.14
2777	7194.86
2810	7187.29
2843	7180
2876	7176.57
2910	7166.29
2944	7160
2977	7153.71
3009	7147.71
3043	7142
3087	7136.29
3116	7130.29
3147	7127
3180	7122
3209	7117.86
3243	7113.43
3277	7107.57
3309	7105
3343	7099.29
3377	7095.43
3410	7091.71
3443	7088.14
3477	7084.57
3510	7081.29
3543	7078

3589	7074.857143
3617	7072.285714
3647	7069.714286
3678	7067
3713	7064.142857
3743	7061.857143
3777	7058.571429
3810	7056.142857
3843	7054
3876	7053
3910	7049.857143
3944	7048
3975	7046.714286
4010	7044.285714
4043	7042.428571
4077	7040.714286
4118	7039.428571
4148	7037.714286
4179	7036.571429
4210	7035.285714
4243	7033.857143
4276	7032.714286
4310	7031.285714
4343	7030.142857
4377	7028.285714
4410	7027.142857
4443	7026
4476	7025
4510	7024
4544	7023
4588	7022
4619	7021.142857
4649	7020.428571
4679	7019.714286
4710	7018.714286
4743	7018.142857
4776	7017.428571
4809	7017
7478	49003

4877	7015.29
4910	7014.71
4944	7014
4977	7013.57
5010	7012.86
5044	7012.29
5089	7011.86
5117	7011.43
5148	7011
5179	7010.57
5215	7009.71
5243	7009.71
5275	7009.43
5309	7009
5342	7008.71
5376	7008.29
5410	7008
5443	7007.71
5476	7007.43
5509	7007.14
5543	7006.71
5589	7006.57
5616	7006.29
5646	7005.71
5681	7005.57
5712	7005.29
5743	7005.14
5776	7004.86
5810	7004.86
5843	7004.43
5876	7004.43
5910	7004.29
5943	7004.14
5977	7003.86
6010	7003.86
6044	7003.71
6087	7003.57
6118	7003.29
8810	21923

6181	7003
6210	7002.86
6243	7002.86
6277	7002.57
6310	7002.71
6343	7002.57
6376	7002.43
6410	7002.43
6443	7002.43
6476	7002.29
6510	7002.14
6543	7002
6587	7001.86
6616	7001.86
6648	7001.86
6682	7001.71
6713	7002
6743	7001.57
6777	7001.57
6810	7001.43
6842	7001.57
6876	7001.57
6910	7001.57
6943	7001.57
6977	7001.43
7010	7001.43
7044	7001.29
7086	7001
7117	7001.29
7149	7001
7180	7001
7212	7001
7243	7000.86
7276	7000.86
7310	7000.86
7342	7001
7310	7000.86
7342	7000.57
7376	7000.86

7411	7000.571429
7444	7000.571429
7478	7000.428571
7511	7000.571429
7544	7000.714286
7586	7000.428571
7635	7000.428571
7652	7000.285714
7684	7000.285714
7712	7000.428571
7745	7000.428571
7777	7000.285714
7810	7000.571429
7860	7000.571429
7900	7000.428571
7944	6983.428571
7977	6935.571429
8011	6855.857143
8044	6748.857143
8085	6589.428571
8117	6455.428571
8152	6303
8182	6168
8214	6017.857143
8244	5874.714286
8276	5721.571429
8309	5626.285714
8344	5399
8374	5298.428571
8410	5083.571429
8443	4923.571429
8475	4819.857143
8510	4600
8544	4435.714286
8588	4221.857143
8621	4063.857143
8650	3919
8682	3762.285714
8743	3462.714286

8877	3295.857143
8925	3131.857143
8962	2963.714286
8992	2800.714286
9024	2636.285714
9055	2377.857143
9083	2271.142857
9118	2066.857143
9144	1951.714286
9189	1774
9212	1599
9243	1464.428571
9275	1244.142857
9309	1095
9335	896.7142857
9364	700.5714286
9397	512.4285714
9428	334.4285714
9460	197.1428571
9489	115.7142857
9520	53.28571429
9553	23.57142857
9593	-1.285714286
9617	-13.57142857
9649	-26
9684	-30.42857143

8,000 RPM Data

Time (ms)	RPM
0	-39
45	-9.28571428
79	21.28571429
103	54.42857143
154	94.85714286
234	93.85714286
271	131.1428571
304	218.8571429
338	350.5714286
384	500.2857143
434	752
471	1020.714286
512	1183.428571
543	1421.285714
574	1596.142857
606	1717.857143
638	1962.571429
671	2146.571429
704	2335.571429
737	2525.285714
771	2714.428571
804	2902.142857
837	3091
870	3278.857143
904	3469.285714
946	3649.714286
981	3835.714286
1010	4004.142857
1039	4173.714286
1076	4371.285714
1105	4538.857143
1137	4692.285714
1170	4876.142857
1203	5047.571429
1236	5243.571429
1270	5513.285714
1304	5694.857143
1337	5875.428571
1371	6055.714286
1404	6233.857143
1437	6407.285714
1521	6788.571429
1617	7101.285714
1635	7155.142857
1664	7236
1699	7345.285714
1728	7408.142857
1758	7447.142857
1790	7501
1824	7556
1854	7596.714286
1887	7631.142857
1921	7683
1954	7713.571429
1987	7727.142857
2021	7764.714286
2054	7785.714286
2086	7804.571429
2121	7821.285714
2154	7836.285714
2188	7849.857143
2227	7864
2258	7874.285714
2289	7880.428571
2325	7890
2355	7897.285714
2387	7903.285714
2420	7910.285714
2454	7919
2487	7924.428571
2521	7929.285714
2552	7932.285714
2587	7938
2620	7941.571429
2654	7945
2700	7948.285714
2730	7951
2758	7953.857143
2792	7955.714286
2823	7957.714286
2853	7959.571429
2887	7962.142857
2921	7964
2954	7965.571429
2987	7966.285714
3021	7968.571429
3054	7969.857143
3087	7971.142857
3121	7972.428571
3154	7973.428571
3187	7974.571429
3230	7975.571429
3259	7976.714286
3291	7977.428571
3322	7978.142857
3353	7979.142857
3386	7979.857143
3419	7980.428571
3454	7981.428571
3487	7982.142857
3520	7982.714286

3554	7983.428571
3587	7984
3621	7984.571429
3654	7985.142857
3688	7985.571429
3729	7986.142857
3758	7986.714286
3789	7987
3820	7987.428571
3853	7987.857143
3886	7988.285714
3919	7988.571429
3953	7989
3986	7989.428571
4020	7990
4054	7990.285714
4087	7990.714286
4120	7991.142857
4166	7991.428571
4198	7991.857143
4229	7992.142857
4260	7992.142857
4289	7992.428571
4325	7992.857143
4355	7993
4386	7993.285714
4420	7993.571429
4453	7993.857143
4487	7994.142857
4521	7994.285714
4554	7994.714286
4587	7994.857143
4620	7995
4653	7995.285714
4687	7995.428571
4730	7995.714286
4759	7995.714286
4790	7996
4820	7996

4854	7996.428571
4887	7996.571429
4920	7996.714286
4954	7997
4987	7997
5021	7997.428571
5052	7997.428571
5087	7997.714286
5121	7997.857143
5154	7998
5188	7998.142857
5229	7998.285714
5258	7998.285714
5290	7998.428571
5321	7998.571429
5355	7998.714286
5386	7998.857143
5420	7998.857143
5454	7999
5487	7999
5521	7999.285714
5554	7999.285714
5587	7999.428571
5621	7999.428571
5654	7999.428571
5699	7999.714286
5729	7999.857143
5761	7999.714286
5790	8000
5825	8000
5856	8000.142857
5886	8000.285714
5920	8000.142857
5954	8000.285714
5986	8000.285714
6020	8000.428571
6054	8000.428571
6087	8000.428571
6121	8000.428571

6154	8000.571429
6199	8000.714286
6231	8000.714286
6259	8000.857143
6291	8000.857143
6323	8000.857143
6353	8000.857143
6386	8001.142857
6420	8001.142857
6454	8001.142857
6486	8001.142857
6521	8001.142857
6553	8001.142857
6587	8001.142857
6620	8001.285714
6654	8001.285714
6699	8001.285714
6729	8001.428571
6758	8001.571429
6789	8001.571429
6820	8001.571429
6857	8001.714286
6886	8001.571429
6920	8001.571429
6953	8001.571429
6986	8001.571429
7021	8001.714286
7054	8001.714286
7087	8001.714286
7120	8001.714286
7154	8001.714286
7197	8001.571429
7229	8001.571429
7258	8001.714286
7288	8001.857143
7324	8001.857143
7354	8001.857143
7387	8001.714286
7420	8001.857143

7454	8001.857143
7487	8001.857143
7520	8001.857143
7553	8002
7587	8001.857143
7620	8001.857143
7654	8001.857143
7699	8002
7728	8001.857143
7761	8001.857143
7792	8001.714286
7821	8001.857143
7856	8001.857143
7887	8001.857143
7921	8002
7954	8002
7987	8002
8051	8002.142857
8073	8002.142857
8104	8002.142857
8137	8002
8171	7984.714286
8204	7933.428571
8238	7848.142857
8271	7737.428571
8304	7612
8338	7475.714286
8371	7333.285714
8404	7186.857143
8449	6986.285714
8478	6854.571429
8510	6708.428571
8540	6569.285714
8583	6411
8621	6194.571429
8654	6038.285714
8699	5823
8729	5678.285714
8761	5523.285714
8790	5382.857143
8825	5214.428571
8854	5127.714286
8887	4919.285714
8920	4757.714286
8954	4596.428571
8987	4436
9021	4275.142857
9053	4113.428571
9087	3949.428571
9120	3786.571429
9154	3624
9200	3447.142857
9230	3299.428571
9260	3151
9292	2998.571429
9323	2845.285714
9353	2700.285714
9387	2541.142857
9420	2381.714286
9454	2139.142857
9487	1972.857143
9520	1806.285714
9554	1638.857143
9587	1471.142857
9620	1302.857143
9654	1103.571429
9699	813.7142857
9729	660.2857143
9760	516.4285714
9792	319.1428571
9821	187.1428571
9856	95.14285714
9886	54.42857143
9920	4.714285714
9954	-10.5714285
9987	-25.1428571
10021	-29.5714285

APPENDIX B

Data for original FESS design:

Weight per inch (lbs)	**1.1125**	**Height (in)**	**4**		**Goal (kWh per day)**	**27.39726027**
ro (in)	ri (in)	ro (m)	ri (m)	r (m)	m (lbs)	m (kg)
1.5	1	0.0381	0.0254	0.03175	4.45	2.018486047
(rpm)	**(rev/s)**	**ω (rad/s)**	**KE (J)**	**KE (kWh)**	**KE (kWh) per day**	**Number of flywheels to reach goal**
6000	100	628.318531	0.194968	5.42E-08	1.29979E-06	21078294.68
7000	116.6667	733.038286	0.227462	6.32E-08	1.51642E-06	18067109.73
8000	133.3333	837.758041	0.259957	7.22E-08	1.73305E-06	15808721.01
9000	150	942.477796	0.292452	8.12E-08	1.94968E-06	14052196.45
10000	166.6667	1047.19755	0.324946	9.03E-08	2.16631E-06	12646976.81
11000	183.3333	1151.91731	0.357441	9.93E-08	2.38294E-06	11497251.64
12000	200	1256.63706	0.389936	1.08E-07	2.59957E-06	10539147.34
13000	216.6667	1361.35682	0.42243	1.17E-07	2.8162E-06	9728443.698
14000	233.3333	1466.07657	0.454925	1.26E-07	3.03283E-06	9033554.863
15000	250	1570.79633	0.48742	1.35E-07	3.24946E-06	8431317.872
16000	266.6667	1675.51608	0.519914	1.44E-07	3.46609E-06	7904360.505
17000	283.3333	1780.23584	0.552409	1.53E-07	3.68273E-06	7439398.122
18000	300	1884.95559	0.584903	1.62E-07	3.89936E-06	7026098.227
19000	316.6667	1989.67535	0.617398	1.71E-07	4.11599E-06	6656303.583

20000	333.3333	2094.3951	0.649893	1.81E-07	4.33262E-06	6323488.404
21000	350	2199.11486	0.682387	1.9E-07	4.54925E-06	6022369.908
22000	366.6667	2303.83461	0.714882	1.99E-07	4.76588E-06	5748625.822
23000	383.3333	2408.55437	0.747377	2.08E-07	4.98251E-06	5498685.569
24000	400	2513.27412	0.779871	2.17E-07	5.19914E-06	5269573.67
25000	416.6667	2617.99388	0.812366	2.26E-07	5.41577E-06	5058790.723
26000	433.3333	2722.71363	0.844861	2.35E-07	5.6324E-06	4864221.849
27000	450	2827.43339	0.877355	2.44E-07	5.84903E-06	4684065.484
28000	466.6667	2932.15314	0.90985	2.53E-07	6.06567E-06	4516777.431
29000	483.3333	3036.8729	0.942344	2.62E-07	6.2823E-06	4361026.485
30000	500	3141.59265	0.974839	2.71E-07	6.49893E-06	4215658.936
31000	516.6667	3246.31241	1.007334	2.8E-07	6.71556E-06	4079669.938
32000	533.3333	3351.03216	1.039828	2.89E-07	6.93219E-06	3952180.252
33000	550	3455.75192	1.072323	2.98E-07	7.14882E-06	3832417.214
34000	566.6667	3560.47167	1.104818	3.07E-07	7.36545E-06	3719699.061
35000	583.3333	3665.19143	1.137312	3.16E-07	7.58208E-06	3613421.945
36000	600	3769.91118	1.169807	3.25E-07	7.79871E-06	3513049.113
37000	616.6667	3874.63094	1.202302	3.34E-07	8.01534E-06	3418101.84
38000	633.3333	3979.35069	1.234796	3.43E-07	8.23197E-06	3328151.792
39000	650	4084.07045	1.267291	3.52E-07	8.44861E-06	3242814.566
40000	666.6667	4188.7902	1.299785	3.61E-07	8.66524E-06	3161744.202

41000	683.3333	4293.50996	1.33228	3.7E-07	8.88187E-06	3084628.49
42000	700	4398.22972	1.364775	3.79E-07	9.0985E-06	3011184.954
43000	716.6667	4502.94947	1.397269	3.88E-07	9.31513E-06	2941157.397
44000	733.3333	4607.66923	1.429764	3.97E-07	9.53176E-06	2874312.911
45000	750	4712.38898	1.462259	4.06E-07	9.74839E-06	2810439.291
46000	766.6667	4817.10874	1.494753	4.15E-07	9.96502E-06	2749342.784
47000	783.3333	4921.82849	1.527248	4.24E-07	1.01817E-05	2690846.129
48000	800	5026.54825	1.559743	4.33E-07	1.03983E-05	2634786.835
49000	816.6667	5131.268	1.592237	4.42E-07	1.06149E-05	2581015.675
50000	833.3333	5235.98776	1.624732	4.51E-07	1.08315E-05	2529395.362
51000	850	5340.70751	1.657226	4.6E-07	1.10482E-05	2479799.374
52000	866.6667	5445.42727	1.689721	4.69E-07	1.12648E-05	2432110.925
53000	883.3333	5550.14702	1.722216	4.78E-07	1.14814E-05	2386222.039
53106.46065	**885.1077**	**5561.29555**	**1.725675**	**4.79E-07**	**1.15045E-05**	**2381438.464**
54000	900	5654.86678	1.75471	4.87E-07	1.16981E-05	2342032.742
55000	916.6667	5759.58653	1.787205	4.96E-07	1.19147E-05	2299450.329
56000	933.3333	5864.30629	1.8197	5.05E-07	1.21313E-05	2258388.716
57000	950	5969.02604	1.852194	5.14E-07	1.2348E-05	2218767.861
58000	966.6667	6073.7458	1.884689	5.24E-07	1.25646E-05	2180513.243
59000	983.3333	6178.46555	1.917184	5.33E-07	1.27812E-05	2143555.391
60000	1000	6283.18531	1.949678	5.42E-07	1.29979E-05	2107829.468
61000	1016.667	6387.90506	1.982173	5.51E-07	1.32145E-05	2073274.887

62000	1033.333	6492.62482	2.014667	5.6E-07	1.34311E-05	2039834.969
63000	1050	6597.34457	2.047162	5.69E-07	1.36477E-05	2007456.636
64000	1066.667	6702.06433	2.079657	5.78E-07	1.38644E-05	1976090.126
65000	1083.333	6806.78408	2.112151	5.87E-07	1.4081E-05	1945688.74
66000	1100	6911.50384	2.144646	5.96E-07	1.42976E-05	1916208.607
67000	1116.667	7016.22359	2.177141	6.05E-07	1.45143E-05	1887608.479
68000	1133.333	7120.94335	2.209635	6.14E-07	1.47309E-05	1859849.531
69000	1150	7225.6631	2.24213	6.23E-07	1.49475E-05	1832895.19
70000	1166.667	7330.38286	2.274624	6.32E-07	1.51642E-05	1806710.973
71000	1183.333	7435.10261	2.307119	6.41E-07	1.53808E-05	1781264.339
72000	1200	7539.82237	2.339614	6.5E-07	1.55974E-05	1756524.557
73000	1216.667	7644.54212	2.372108	6.59E-07	1.58141E-05	1732462.576
74000	1233.333	7749.26188	2.404603	6.68E-07	1.60307E-05	1709050.92
75000	1250	7853.98163	2.437098	6.77E-07	1.62473E-05	1686263.574
75028.28329	**1250.471**	**7856.94345**	**2.438017**	**6.77E-07**	**1.62534E-05**	**1685627.906**
76000	1266.667	7958.70139	2.469592	6.86E-07	1.64639E-05	1664075.896

Max Stress for 1026 Carbon Steel **490 Mpa**

Inertia (kg*m^2)		
0.000620602		
ρ, density (kg/m^3)	**Max Stress, σ (Pa)**	**Max Stress, σ (MPa)**
7858	3127225.656	3.127225656
7858	4256501.588	4.256501588
7858	5559512.278	5.559512278
7858	7036257.726	7.036257726
7858	8686737.934	8.686737934
7858	10510952.9	10.5109529
7858	12508902.62	12.50890262
7858	14680587.11	14.68058711
7858	17026006.35	17.02600635
7858	19545160.35	19.54516035
7858	22238049.11	22.23804911
7858	25104672.63	25.10467263
7858	28145030.91	28.14503091
7858	31359123.94	31.35912394
7858	34746951.74	34.74695174
7858	38308514.29	38.30851429
7858	42043811.6	42.0438116
7858	45952843.67	45.95284367
7858	50035610.5	50.0356105
7858	54292112.09	54.29211209
7858	58722348.43	58.72234843
7858	63326319.54	63.32631954
7858	68104025.4	68.1040254
7858	73055466.02	73.05546602
7858	78180641.4	78.1806414
7858	83479551.54	83.47955154
7858	88952196.44	88.95219644
7858	94598576.1	94.5985761

7858	100418690.5	100.4186905
7858	106412539.7	106.4125397
7858	112580123.6	112.5801236
7858	118921442.3	118.9214423
7858	125436495.8	125.4364958
7858	132125284	132.125284
7858	138987806.9	138.9878069
7858	146024064.7	146.0240647
7858	153234057.2	153.2340572
7858	160617784.4	160.6177844
7858	168175246.4	168.1752464
7858	175906443.2	175.9064432
7858	183811374.7	183.8113747
7858	191890041	191.890041
7858	200142442	200.142442
7858	208568577.8	208.5685778
7858	217168448.3	217.1684483
7858	225942053.7	225.9420537
7858	234889393.7	234.8893937
7858	244010468.6	244.0104686
7858	**244991736.6**	**244.9917366**
7858	253305278.1	253.3052781
7858	262773822.5	262.7738225
7858	272416101.6	272.4161016
7858	282232115.5	282.2321155
7858	292221864.1	292.2218641
7858	302385347.5	302.3853475
7858	312722565.6	312.7225656
7858	323233518.5	323.2335185
7858	333918206.2	333.9182062
7858	344776628.6	344.7766286
7858	355808785.8	355.8087858
7858	367014677.7	367.0146777
7858	378394304.4	378.3943044
7858	389947665.8	389.9476658
7858	401674762.1	401.6747621
7858	413575593	413.575593
7858	425650158.8	425.6501588
7858	437898459.2	437.8984592
7858	450320494.5	450.3204945

7858	462916264.5	462.9162645
7858	475685769.3	475.6857693
7858	488629008.8	488.6290088
7858	488997612.6	488.9976126
7858	501745983.1	501.7459831

rpm	Max Stress, σ (MPa)	Energy produced (kWh) per day
53000	244.0104686	1.14814E-05
53106.46	245	1.15045E-05
54000	253.3052781	1.16981E-05

rpm	Max Stress, σ (MPa)	Energy produced (kWh) per day
75000	488.6290088	1.62473E-05
75028.28	**489**	**1.62534E-05**
76000	501.7459831	1.64639E-05

Data for FESS design #2:

Weight per inch (lbs)	**9.7917**	**Height (in)**	**48**	**Volume (in^3)**	**38000.7**	
ro (in)	ri (in)	ro (m)	ri (m)	r (m)	Volume (m^3)	m (lbs)
24	18	0.6096	0.4572	0.5334	0.62272	4893.334
(rpm)	**(rev/s)**	**ω (rad/s)**	**KE (J)**	**KE (kWh)**	**KE (kWh per day)**	**Number of flywheels to reach goal**
100	1.666667	10.4719755	1008.498	0.000280138	0.006723	4074.96
400	6.666667	41.887902	4033.992	0.001120553	0.026893	1018.74
700	11.66667	73.3038286	7059.486	0.001960968	0.047063	582.1371
1000	16.66667	104.719755	10084.98	0.002801383	0.067233	407.496
1300	21.66667	136.135682	13110.47	0.003641798	0.087403	313.4585
1600	26.66667	167.551608	16135.97	0.004482213	0.107573	254.685
1900	31.66667	198.967535	19161.46	0.005322628	0.127743	214.4716
2200	36.66667	230.383461	22186.96	0.006163043	0.147913	185.2255
2500	41.66667	261.799388	25212.45	0.007003458	0.168083	162.9984
2800	46.66667	293.215314	28237.94	0.007843873	0.188253	145.5343

3100	51.66667	324.631241	31263.44	0.008684289	0.208423	131.4503
3158.905072	**52.64842**	**330.799766**	**31857.5**	**0.008849304**	**0.212383**	**128.9991**
3400	56.66667	356.047167	34288.93	0.009524704	0.228593	119.8518
3700	61.66667	387.463094	37314.43	0.010365119	0.248763	110.1341
4000	66.66667	418.87902	40339.92	0.011205534	0.268933	101.874
4300	71.66667	450.294947	43365.41	0.012045949	0.289103	94.76651
453.3276347	**7.555461**	**47.4723589**	**4571.8**	**0.001269945**	**0.030479**	**898.8995**
4600	76.66667	481.710874	46390.91	0.012886364	0.309273	88.58609

Goal (kWh per day)	**27.39726027**	**Max Stress for 1026 Carbon Steel**	**490 Mpa**

m (kg)	Inertia (kg*m^2)	
2219.578788	192.6089341	
ρ, density (kg/m^3)	**Max Stress, σ (Pa)**	**Max Stress, σ (MPa)**
7858	245174.4914	0.245174491
7858	3922791.863	3.922791863
7858	12013550.08	12.01355008
7858	24517449.14	24.51744914
7858	41434489.05	41.43448905
7858	62764669.81	62.76466981
7858	88507991.41	88.50799141
7858	118664453.9	118.6644539
7858	153234057.2	153.2340572
7858	192216801.3	192.2168013
7858	235612686.3	235.6126863
7858	**244651810.2**	**244.6518102**
7858	283421712.1	283.4217121
7858	335643878.8	335.6438788
7858	392279186.3	392.2791863
7858	453327634.7	453.3276347
7858	**5038481.54**	**5.03848154**
7858	518789223.9	518.7892239

Interpolation				Interpolation		
rpm	**Max Stress, σ (MPa)**	**Energy produced (kWh) per day**		**rpm**	**Max Stress, σ (MPa)**	**Energy produced (kWh) per day**
3100	235.6126863	0.208423		4300	453.3276347	0.289103
3158.905072	**245**	**0.212383**		**4468.063589**	**490**	**0.030479**
3400	283.4217121	0.228593		4600	518.7892239	0.309273

Data for FESS design #3:

Weight per inch (lbs)	**1.538**	**Height (in)**	**4**	**Volume (in^3)**	**15.707963**	
ro (in)	ri (in)	ro (m)	ri (m)	r (m)	Volume (m^3)	m (kg)
1.5	1	0.0381	0.0254	0.03175	0.0002574	0.413138876
(rpm)	**(rev/s)**	**ω (rad/s)**	**KE (J)**	**KE (kWh)**	**KE (kWh) per day**	**Number of FESS to reach goal**
10000	166.6667	1047.19755	0.20644	5.73445E-08	1.376E-06	19906910.89
15000	250	1570.79633	0.30966	8.60168E-08	2.064E-06	13271273.92
20000	333.3333	2094.3951	0.412881	1.14689E-07	2.753E-06	9953455.443
25000	416.6667	2617.99388	0.516101	1.43361E-07	3.441E-06	7962764.354
30000	500	3141.59265	0.619321	1.72034E-07	4.129E-06	6635636.962
35000	583.3333	3665.19143	0.722541	2.00706E-07	4.817E-06	5687688.825
40000	666.6667	4188.7902	0.825761	2.29378E-07	5.505E-06	4976727.722
45000	750	4712.38898	0.928981	2.5805E-07	6.193E-06	4423757.975
50000	833.3333	5235.98776	1.032202	2.86723E-07	6.881E-06	3981382.177
55000	916.6667	5759.58653	1.135422	3.15395E-07	7.569E-06	3619438.343
60000	1000	6283.18531	1.238642	3.44067E-07	8.258E-06	3317818.481
65000	1083.333	6806.78408	1.341862	3.72739E-07	8.946E-06	3062601.675
70000	1166.667	7330.38286	1.445082	4.01412E-07	9.634E-06	2843844.412
75000	1250	7853.98163	1.548302	4.30084E-07	1.032E-05	2654254.785
80000	1333.333	8377.58041	1.651523	4.58756E-07	1.101E-05	2488363.861
85000	1416.667	8901.17919	1.754743	4.87429E-07	1.17E-05	2341989.516

90000	1500	9424.77796	1.857963	5.16101E-07	1.239E-05	2211878.987
95000	1583.333	9948.37674	1.961183	5.44773E-07	1.307E-05	2095464.304
100000	**1666.667**	**10471.9755**	**2.064403**	**5.73445E-07**	**1.376E-05**	**1990691.089**

Goal (kWh per day) **27.39726027** **UTS of T1000G/epoxy** **8577.50 Mpa**

Inertia (kg*m^2)			
0.000394272			
ρ, density (kg/m^3)	**Max Stress, σ (Pa)**	**Max Stress, σ (MPa)**	
1605	1774270.092	1.774270092	
1605	3992107.707	3.992107707	
1605	7097080.368	7.097080368	
1605	11089188.08	11.08918808	
1605	15968430.83	15.96843083	
1605	21734808.63	21.73480863	
1605	28388321.47	28.38832147	
1605	35928969.37	35.92896937	
1605	44356752.3	44.3567523	
1605	53671670.29	53.67167029	
1605	63873723.32	63.87372332	
1605	74962911.39	74.96291139	
1605	86939234.51	86.93923451	
1605	99802692.68	99.80269268	
1605	113553285.9	113.5532859	
1605	128191014.2	128.1910142	
1605	143715877.5	143.7158775	
1605	160127875.8	160.1278758	
1605	**177427009.2**	**177.4270092**	

Data for FESS design #4:

Height (in)	**48**	**Volume (in^3)**	**38000.7**

ro (in)	ri (in)	ro (m)	ri (m)	r (m)	Volume (m^3)	m (kg)
24	18	0.6096	0.4572	0.5334	0.62272	999.4655688
(rpm)	**(rev/s)**	**ω (rad/s)**	**KE (J)**	**KE (kWh)**	**KE (kWh) per day**	**Number of flywheels to reach goal**
10000	166.6667	1047.198	140956.4195	0.039155	0.939709	29.15503285
15000	250	1570.796	211434.6293	0.058732	1.409564	19.43668856
20000	333.3333	2094.395	281912.839	0.078309	1.879419	14.57751642
25000	416.6667	2617.994	352391.0488	0.097886	2.349274	11.66201314
29207.8384	**486.7973**	**3058.638**	**411703.2322**	**0.114362**	**2.744688**	**9.981920761**
30000	500	3141.593	422869.2586	0.117464	2.819128	9.718344282
35000	583.3333	3665.191	493347.4683	0.137041	3.288983	8.330009385
40000	666.6667	4188.79	563825.6781	0.156618	3.758838	7.288758212
41327.79087	**688.7965**	**4327.836**	**582541.7427**	**0.161817**	**3.883612**	**7.054582942**
45000	750	4712.389	634303.8878	0.176196	4.228693	6.478896188
50000	833.3333	5235.988	704782.0976	0.195773	4.698547	5.831006569
55000	916.6667	5759.587	775260.3074	0.21535	5.168402	5.300915063
60000	1000	6283.185	845738.5171	0.234927	5.638257	4.859172141
65000	1083.333	6806.784	916216.7269	0.254505	6.108112	4.485389669
70000	1166.667	7330.383	986694.9366	0.274082	6.577966	4.165004692
75000	1250	7853.982	1057173.146	0.293659	7.047821	3.887337713
80000	1333.333	8377.58	1127651.356	0.313236	7.517676	3.644379106
85000	1416.667	8901.179	1198129.566	0.332814	7.98753	3.430003864
90000	1500	9424.778	1268607.776	0.352391	8.457385	3.239448094
95000	1583.333	9948.377	1339085.985	0.371968	8.92724	3.068950826
100000	1666.667	10471.98	1409564.195	0.391546	9.397095	2.915503285

Goal (kWh per day)	**27.39726027**	**UTS of T1000G/epoxy (Mpa)**	**8577.5**
Inertia (kg*m^2)			
269.2069311			
ρ, density (kg/m^3)	**Max Stress, σ (Pa)**	**Max Stress, σ (MPa)**	
1605	500769990.8	500.7699908	
1605	1126732479	1126.732479	
1605	2003079963	2003.079963	
1605	3129812442	3129.812442	
1605	**4272057894**	**4272.057894**	
1605	4506929917	4506.929917	
1605	6134432387	6134.432387	
1605	8012319853	8012.319853	
1605	**8553082827**	**8553.082827**	
1605	10140592314	10140.59231	
1605	12519249770	12519.24977	
1605	15148292222	15148.29222	
1605	18027719669	18027.71967	
1605	21157532111	21157.53211	
1605	24537729549	24537.72955	
1605	28168311982	28168.31198	
1605	32049279411	32049.27941	
1605	36180631835	36180.63184	
1605	40562369254	40562.36925	
1605	45194491669	45194.49167	
1605	50076999080	50076.99908	

Interpolation

rpm	Max Stress, σ (MPa)	Energy produced (kWh) per day
25000	3129.812442	2.349273659
29207.8384	4288.75	2.744688215
30000	4506.929917	2.81912839

Interpolation

rpm	Max Stress, σ (MPa)	Energy produced (kWh) per day
40000	8012.319853	3.758837854
41327.79087	**8577.5**	**3.883611618**
45000	10140.59231	4.228692586

REFERENCES

[1] "History of flywheel energy storage systems | Gerotor AG," *Gerotor GmbH | Aktives Energiemanagement*. http://gerotor.tech/history-of-flywheel-energy-storage-systems/ (accessed Apr. 05, 2019).

[2] Mustafa E. Amiryar and Keith R. Pullen, "A Review of Flywheel Energy Storage System Technologies and Their Applications," *Appl. Sci. MDPI*, Dec. 2016.

[3] A. Dhabi, "Renewable Energy Now Accounts for a Third of Global Power Capacity," *https://www.irena.org/newsroom/pressreleases/2019/Apr/Renewable-Energy-Now-Accounts-for-a-Third-of-Global-Power-Capacity*, Apr. 02, 2019. /newsroom/pressreleases/2019/Apr/Renewable-Energy-Now-Accounts-for-a-Third-of-Global-Power-Capacity (accessed Apr. 03, 2019).

[4] K. Thoubboron, "What's the cheapest time of day to use electricity with time-of-use rates?," *Solar News*, Jul. 09, 2018. https://news.energysage.com/whats-the-cheapest-time-of-day-to-use-electricity-with-time-of-use-rates/ (accessed Apr. 24, 2020).

[5] "Time-of-Day (5-8 p.m.) Rate." https://www.smud.org/en/Rate-Information/Time-of-Day-rates/Time-of-Day-5-8pm-Rate (accessed Mar. 21, 2020).

[6] "FAQs," *SMUD*. https://www.smud.org/en/Rate-Information/Time-of-Day-rates/Time-of-Day-5-8pm-Rate/Time-of-Day-FAQs (accessed Apr. 24, 2020).

[7] S. Mullendore, "Closing the Clean Energy Divide with Solar+Storage," *Clean Energy Group*, May 19, 2016. https://www.cleanegroup.org/closing-clean-energy-divide-solarstorage/ (accessed Apr. 24, 2020).

[8] D. Roberts, “Solar power’s greatest challenge was discovered 10 years ago. It looks like a duck.,” *Vox*, Mar. 20, 2018. https://www.vox.com/energy-and-environment/2018/3/20/17128478/solar-duck-curve-nrel-researcher (accessed Apr. 24, 2020).

[9] B. Jones-Albertus, “Confronting the Duck Curve: How to Address Over-Generation of Solar Energy,” *Energy.gov*, Oct. 12, 2017. https://www.energy.gov/eere/articles/confronting-duck-curve-how-address-over-generation-solar-energy (accessed Apr. 24, 2020).

[10] POWER, “Developments in Energy Storage Could Spell the End of the Duck Curve,” *POWER Magazine*, Jun. 01, 2018. https://www.powermag.com/developments-in-energy-storage-could-spell-the-end-of-the-duck-curve/ (accessed Apr. 24, 2020).

[11] R. Hudson and G. Heilscher, “PV Grid Integration – System Management Issues and Utility Concerns,” *Energy Procedia*, vol. 25, pp. 82–92, 2012, doi: 10.1016/j.egypro.2012.07.012.

[12] Biologydictionary.net Editors, “What is Solar Irradiance | Biology Dictionary,” *Biology Dictionary*. https://biologydictionary.net/what-is-solar-irradiance/ (accessed Mar. 22, 2020).

[13] V. Salehi and B. Radibratovic, “Ramp rate control of photovoltaic power plant output using energy storage devices,” in *2014 IEEE PES General Meeting | Conference Exposition*, Jul. 2014, pp. 1–5, doi: 10.1109/PESGM.2014.6938985.

[14] Solar Power Authority Staff, “How to Calculate Your Peak Sun-Hours,” *Solar Power Authority*, Mar. 18, 2016. https://www.solarpowerauthority.com/how-to-calculate-your-peak-sun-hours/ (accessed Mar. 22, 2020).

[15] “Load Shifting Battery - Adelaide EcoSouth,” *Adelaide EcoSouth*. https://www.ecosouth.com.au/index.php/systems/load-shifting-battery (accessed Mar. 22, 2020).

[16] “What are TOU rates?,” *California Public Utilites Commission*. https://www.cpuc.ca.gov/General.aspx?id=12194 (accessed Apr. 25, 2020).

[17] Sunrun, “What are tiered utility rates?,” *Sunrun*, Dec. 05, 2017. https://www.sunrun.com/go-solar-center/solar-faq/what-are-tiered-utility-rates (accessed Apr. 25, 2020).

[18] “Products – Amber Kinetics,” *Amber Kinetics*. https://www.amberkinetics.com/products/ (accessed Apr. 24, 2020).

[19] Energy Storage Report, “Amber Kinetics: new model next year,” *Energy Storage Report*, Oct. 04, 2017. http://energystoragereport.info/amber-kinetics-flywheel-sales-next-year/ (accessed Apr. 24, 2020).

[20] Michal Smolinski, Tomasz Perkowski, Arkadiusz Mystkowski, Egidijus Dragasius, Darius Eidukynas, and Rafal P. Jastrzebski, “AMB Flywheel Integration with Photovoltaic System for Household Purpose – Modeling and Analysis,” *ResearchGate*, vol. 19, no. 1, 2017.

[21] EcoFriendlyLink, “Batteries and Their Effects on the Environment - EcoFriendlyLink,” *EcoFriendlyLink - Naturally Healthy Green Living*, Dec. 19,

2017. http://www.ecofriendlylink.com/blog/batteries-and-the-environment/ (accessed Mar. 22, 2020).

[22] Robert E. Hebner, Joseph H. Beno, and Alan Walls, "Flywheel Batteries Come Around Again," *IEEE Spectr.*, vol. 39, no. 4, pp. 46–51, Apr. 2002.

[23] R. vor dem Esche, "Safety of Flywheel Storage Systems," Oct. 2016, doi: 10.13140/RG.2.2.12482.99524.

[24] S. Bankston and C. Mo, "Geometry Modification of Flywheels and its Effect on Energy Storage," *Energy Res. J.*, vol. 6, no. 2, pp. 54–63, Feb. 2015, doi: 10.3844/erjsp.2015.54.63.

[25] "Mass Moment of Inertia," *Engineering Toolbox*. https://www.engineeringtoolbox.com/moment-inertia-torque-d_913.html (accessed Apr. 05, 2020).

[26] "Stress in Thin-Walled Tubes or Cylinders," *Engineering Toolbox*. https://www.engineeringtoolbox.com/stress-thin-walled-tube-d_948.html (accessed Apr. 05, 2020).

[27] "10.7 Newton's Second Law for Rotation | University Physics Volume 1," *University Physics*. https://courses.lumenlearning.com/suny-osuniversityphysics/chapter/10-7-newtons-second-law-for-rotation/ (accessed Mar. 28, 2020).

[28] S. Gurumurthy, V. Agarwal, and A. Sharma, "Design considerations for a PM-BLDC machine for flywheel energy storage applications," presented at the 2015

IEEE 6th International Symposium on Power Electronics for Distributed Generation Systems (PEDG), Jun. 2015, pp. 1–8, doi: 10.1109/PEDG.2015.7223075.

[29] B. Rojas-Delgado, M. Alonso, H. Amaris, and J. Santiago, “Wave Power Output Smoothing through the Use of a High-Speed Kinetic Buffer,” *Energies*, vol. 12, p. 2196, Jun. 2019, doi: 10.3390/en12112196.

[30] T. Abuzairi, W. W. A. Ramadhan, and K. Devara, “Solar Charge Controller with Maximum Power Point Tracking for Low-Power Solar Applications,” *Int. J. Photoenergy*, vol. 2019, p. e5026464, Oct. 2019, doi: 10.1155/2019/5026464.

[31] A. K. Singh, A. Agrawal, S. Vohra, S. S. Thakur, and G. R. Patel, “Solar charge controller,” *Int. J. Acad. Res. Dev.*, vol. 2, no. 6, pp. 994–1001, Nov. 2017.

[32] “Y SOLAR PWM 60A 50A 40A 30A 20A 10A Solar Charge and Discharge Controller 12V 24V Auto LCD Solar Regulator with Dual USB 5V,” *aliexpress.com*. //www.aliexpress.com/item/32944689428.html?src=ibdm_d03p0558e02r02&sk=&aff_platform=&aff_trace_key=&af=&cv=&cn=&dp= (accessed Apr. 26, 2020).

[33] VESC Team, “VESC Tool,” *VESC Project*. https://vesc-project.com/vesc_tool (accessed Mar. 25, 2020).

[34] “Enertion FOCBOX,” *Street Wing Electric Skateboards and Parts - ESK8 Professionals*. https://street-wing.com/product/enertion-focbox-vesc-x/ (accessed Mar. 25, 2020).

[35] S. Jain and L. Kumar, “Fundamentals of Power Electronics Controlled Electric Propulsion,” in *Power Electronics Handbook*, Elsevier, 2018, pp. 1023–1065.

[36] Y. Shao, X. Wang, Q. Gao, and Y. Li, “Rotor Strength Analysis of Ultra-High Speed Permanent Magnet synchronous Motor,” in *2019 22nd International Conference on Electrical Machines and Systems (ICEMS)*, Aug. 2019, pp. 1–4, doi: 10.1109/ICEMS.2019.8922108.

[37] D. Ouamara and F. Dubas, “Permanent-Magnet Eddy-Current Losses: A Global Revision of Calculation and Analysis,” *Math. Comput. Appl.*, vol. 24, no. 3, p. 67, Sep. 2019, doi: 10.3390/mca24030067.

[38] E. Schmidt, M. Kaltenbacher, and A. Wolfschluckner, “Eddy current losses in permanent magnets of surface mounted permanent magnet synchronous machines—Analytical calculation and high order finite element analyses,” *E Elektrotechnik Informationstechnik*, vol. 134, no. 2, pp. 148–155, Apr. 2017, doi: 10.1007/s00502-017-0498-y.

[39] E. E. Kriezis, T. D. Tsiboukis, S. M. Panas, and J. A. Tegopoulos, “Eddy currents: theory and applications,” *Proc. IEEE*, vol. 80, no. 10, pp. 1559–1589, Oct. 1992, doi: 10.1109/5.168666.

[40] A. M. Welekar and A. A. Apte, “Development of Brushless DC Motor Drive,” *IOSR J. Electr. Electron. Eng.*, p. 7.

[41] “APS 6374S Sensored Outrunner brushless motor 400KV 3200W,” *Alien Power System*. https://alienpowersystem.com/shop/brushless-motors/63mm/aps-6374s-sensored-outrunner-brushless-motor-400kv-3200w/ (accessed May 12, 2019).

[42] F. Nadeem, S. Hussain, P. Tiwari, A. Goswami, and T. S. Ustun, “Comparative Review of Energy Storage Systems, Their Roles and Impacts on Future Power

Systems," *IEEE Access*, vol. 7, pp. 4555–4585, Jan. 2019, doi: 10.1109/ACCESS.2018.2888497.

[43] C. Liu, P. Liu, Z. Zhao, and D. O. Northwood, "Room temperature creep of a high strength steel," *ResearchGate*, Mar. 2000, Accessed: Mar. 26, 2020. [Online].

[44] R. L. Norton, "Chapter 10 Bearings and Lubrication," in *Machine Design an Integrated Approach*, 5th ed., Prentice Hall, 2013, pp. 612–619.

[45] "Passive Bearings," *Magnetic Bearings*. http://www.magneticbearings.org/technology-2/technologies/passive-bearings/ (accessed Mar. 28, 2020).

[46] "Vacuum Chamber | Labx," *LabX*. https://www.labx.com/product/vacuum-chamber (accessed Apr. 25, 2020).

[47] N. E. Dowling, *Mechanical Behavior of Materials*, 4th ed. Pearson, 2012.

[48] "System Installation," *Beacon Power*. https://beaconpower.com/system-installation/ (accessed Apr. 12, 2020).

[49] "Amber Kinetics: M32 Flywheel Installation & Maintenance Manual." Amber Kinetics, Mar. 2018.

[50] J. Sajip, "What Determines the Rotating Speed of a Motor?" https://www.ny-engineers.com/blog/what-determines-the-rotating-speed-of-a-motor (accessed Apr. 25, 2020).

[51] "5. Additional settings: Throttle curves, ERPM limits, safety features etc. | VESC Project," *VESC Project*. https://vesc-project.com/node/183 (accessed Apr. 13, 2020).

[52] AZoM, “AISI 1026 Carbon Steel (UNS G10260),” *AZoM.com*, Aug. 28, 2012. https://www.azom.com/article.aspx?ArticleID=6583 (accessed Apr. 05, 2020).

[53] “Carbon Steel Grade 1026 | Elgin Fasteners.” https://elginfasteners.com/resources/materials/material-specifications/carbon-steel-grade-1026/ (accessed Apr. 06, 2020).

[54] “Stephentown, New York | Beacon Power.” https://beaconpower.com/stephentown-new-york/ (accessed Apr. 09, 2020).

[55] J. Sloan, “Composites 101: Fibers and resins,” *Composites World*, Mar. 14, 2016. https://www.compositesworld.com/articles/composites-101-fibers-and-resins (accessed Apr. 10, 2020).

[56] “Toray Composite Materials America, Inc.,” *Toray Composite Materials America, Inc.* https://www.toraycma.com/page.php?id=661 (accessed Apr. 12, 2020).

[57] P. Breeze, “Chapter 6 - Flywheels,” in *Power System Energy Storage Technologies*, P. Breeze, Ed. Academic Press, 2018, pp. 53–59.

[58] M. A. Conteh and E. C. Nsofor, “Composite flywheel material design for high-speed energy storage,” Oct. 2015.

[59] K. A. Germany Frankenthal, “Critical speed,” *KSB*. https://www.ksb.com/centrifugal-pump-lexicon/ (accessed Apr. 13, 2020).

[60] K. Tweed, “Quantum Energy Storage Redesigns the Flywheel for Microgrids,” Aug. 10, 2015. https://www.greentechmedia.com/articles/read/quantum-energy-storage-redesigns-the-flywheel-for-microgrids (accessed Apr. 13, 2020).